HISTOLOGIC®
Technical Bulletin for Histotechnology

Fig. 1. Single photon emission computerized tomography. A) Altered blood circulation in an AD brain. B) Normal brain.

A Brief Review of Alzheimer's Disease by Using Conventional Silver Staining Procedures

Dr. Alicia A. Zuniga, CLS, HTL (ASCP); Patricia Gonzalez, BS, HT;
Antonio Fernandez, MD
School of Natural and Health Sciences
Barry University, Miami Shores, FL
azuniga@mail.barry.edu

Abstract
Alzheimer's Disease (AD) is the leading cause of dementia. As many as 10% of all people 65 years of age and older have AD, and as many as 50% of those 85 and older have the disease. The high morbidity and mortality associated with this disorder and its increasing prevalence in aging populations require the histology laboratory to have in its arsenal reproducible staining methods to render this diagnosis in biopsy sections. We evaluated different silver stains to identify which is most useful for making the diagnosis of AD in histological sections. We found that the Bielschowsky silver stain is the best method to demonstrate AD pathology in our laboratory. The senile or neuritic plaques were the most conspicuous histologic lesion observed in sections stained with the Bielschowsky technique.

Introduction
Alzheimer's disease is a slowly progressive cerebral degeneration characterized by dementia. Increasing age and the presence of the beta-amyloid protein in neuritic plaques are risk factors associated with AD.[1] Extensive research is ongoing in an attempt to better understand AD. The following theories have been proposed for its etiology: invasion by slow viruses, acetylcholinesterase deficiency, aluminum excess, autoimmune responses, genetic predisposition, amyloid protein deposition, and vascular changes. In patients with AD, neurons and neuritic processes are lost. The gyri narrow, the sulci widen, and cortical atrophy becomes apparent (Fig. 2B).[1]

A common finding in the brains of Alzheimer's disease patients is a loss of approximately 200 g in a span of 3 to 8 years. The atrophy is bilateral and symmetric and targets the frontal and hippocampal cortex (Fig. 2). A definitive Alzheimer's diagnosis is based on large
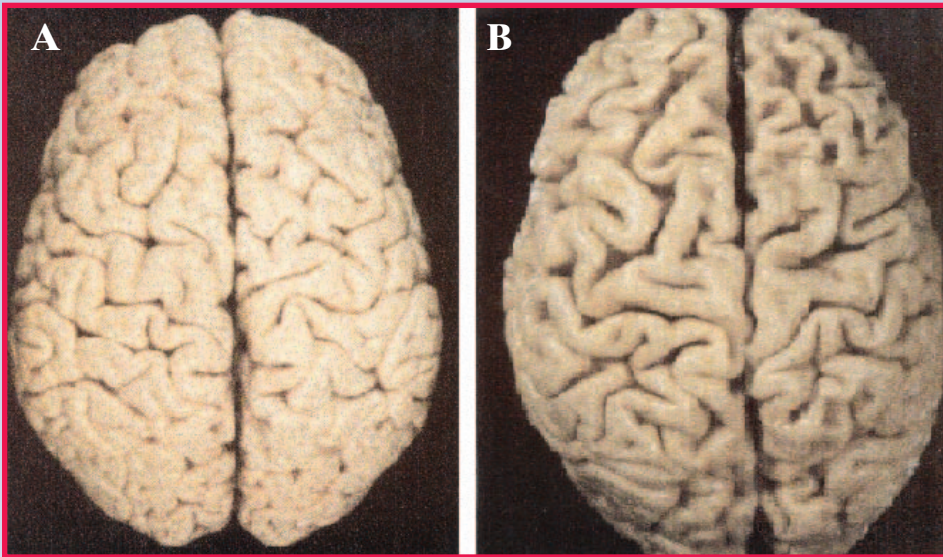
Fig. 2A. Normal brain.

Fig. 2B. The brain of a patient with AD shows cortical atrophy, characterized by slender gyri and prominent sulci.

water, collected onto precleaned, charged slides, and dried overnight in a 39°C oven, deparaffinized, and rehydrated to distilled water prior to staining. Staining techniques included the Bielschowsky silver stain, Bodian silver stain, hematoxylin & eosin, and a modification of the methenamine silver stain, using both microwave and conventional procedures.

Slides were observed under a light microscope and cortical areas were selected at 40X, 100X, and 400X magnifications using the DP12 Olympus® Microscope Digital Camera System (Olympus America, Melville, NY). The pictures recorded in the SmartMedia™ installed in the camera system were viewed with the software provided with the DP12-BSW. Saved pictures were printed using a Hewlett Packard Deskjet 660 color printer.

numbers of microscopic neurofibrillary tangles, neuropil threads, neuritic plaques, and granulovacuolar degeneration present in several tissue samples of cerebral cortex. Symptoms include loss of memory, judgment and reasoning, difficulty with day-to-day function, and changes in mood and behavior. The utilization of imaging studies in the diagnosis of AD is done mainly to exclude structural lesions such as subdural hemorrhage and brain tumors. Figure 1 shows a single photon emission computerized tomography indicating how blood is circulating in normal (B) and AD brain (A).

We evaluated the Bielschowsky silver stain, Bodian silver stain, and modifications of the methenamine silver stain for the utility in demonstrating microscopic changes in brains from patients with Alzheimer's disease.

Materials and Methods
Brain samples from three patients who died from cardiorespiratory failure and had a history of progressive cognitive decline were fixed in 10% buffered formalin for 14 days. Several tissue blocks from each case were cut on a rotary microtome. Sections of 8-10 μ were floated on a water bath at 41°-43°C in distilled

Results
The preliminary results of this overview indicate that the Bielschowsky silver stain[2] is the best staining method used in our laboratory to demonstrate AD pathology. The conventional procedure was compared to the microwave modification.[3] The two techniques differed in the amount of time employed to do the procedures but results were
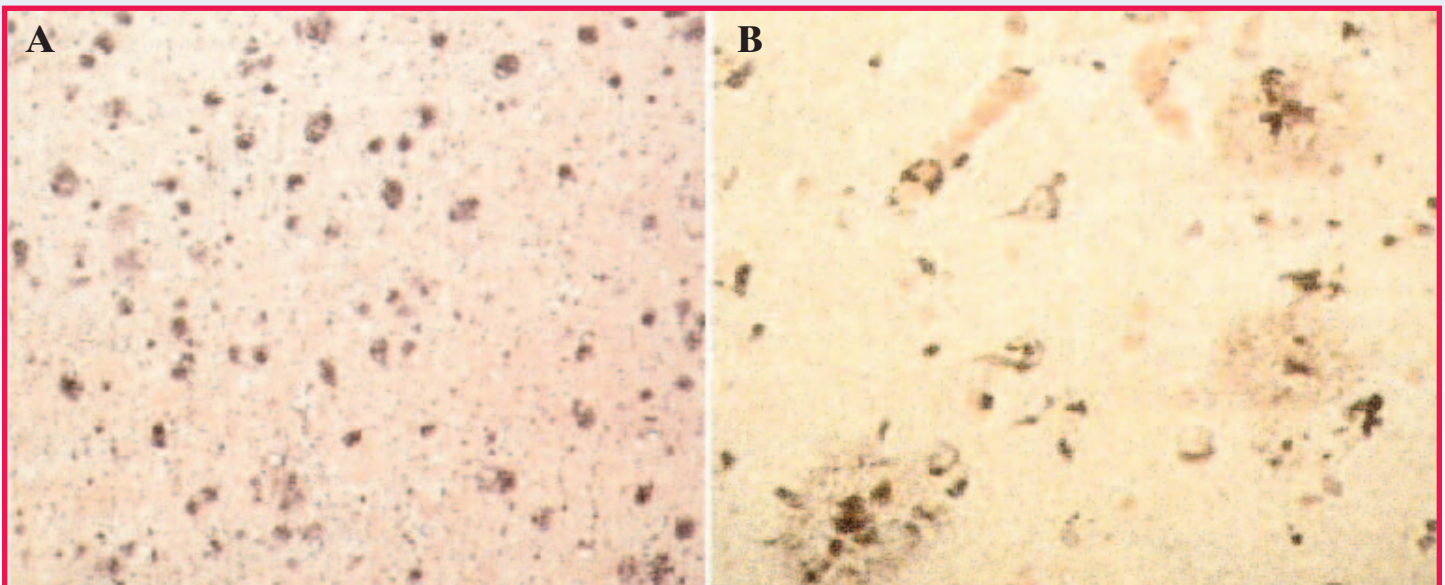

Fig. 3A. Section of cerebral cortex revealing the presence of neuritic plaques. H&E, 40X

Fig. 3B. At higher magnification, the uniform size and spherical shape of the neuritic plaques are observed. Silver stain, 100X
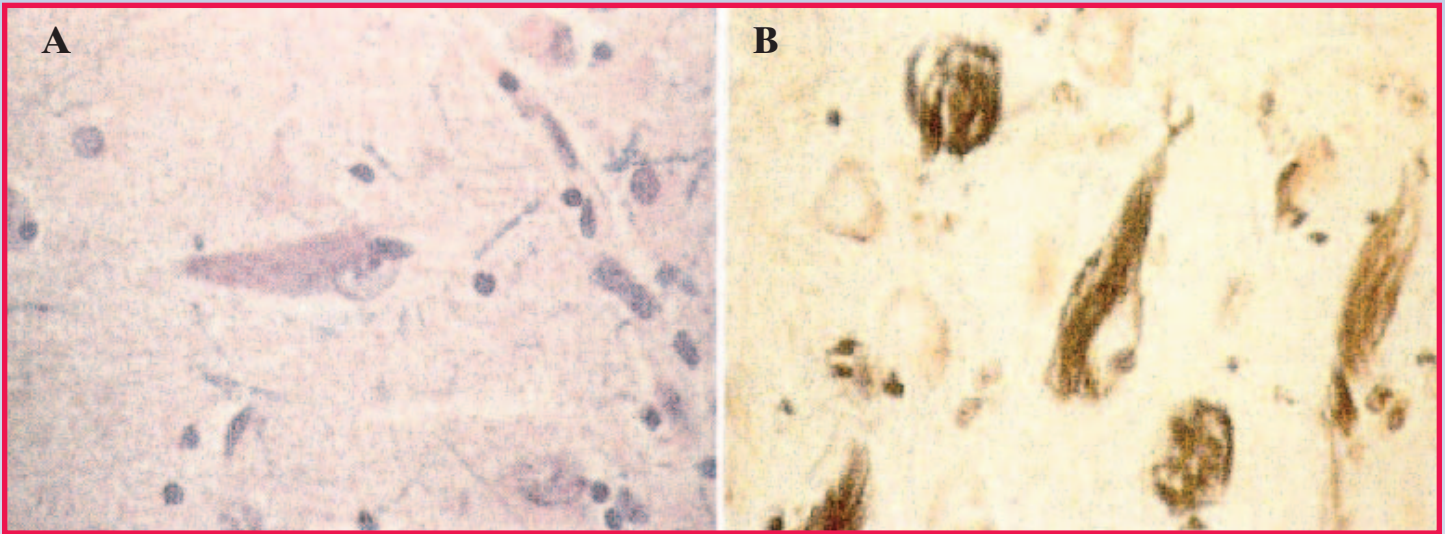
Fig. 4A. The cytoplasm of a neuron is distended by neurofibrillary tangles. H&E, 100X

Fig. 4B. A Bielschowsky silver stain demonstrates the fibrillary character of the cytoplasmic inclusions. 100X

conclusive in both. The major microscopic features observed in the sections of cortex from patients with Alzheimer's disease were neurofibrillary tangles and neuritic plaques (Figs. 3, 4). The neurofibrillary tangles found within the cytoplasm of abnormal neurons consist of fibrous proteins that are wound around each other as pairs of helical filaments. The main component of tangles[1] (Fig. 4A, 4B) is an abnormal phosphorylated form of a normally occurring microtubule-associated protein (MAP), termed tau, which is necessary to stabilize neuronal microtubules for proper axonal transport. The abnormally phosphorylated tau is less able to bind microtubules, probably causing microtubule depolymerization, disrupted axonal transport, compromised synaptic neurotransmission, and finally, neuronal death. These tangles are resistant to chemical and enzymatic breakdown, and they persist in brain tissue long after the neuron in which they arose has died and disappeared. The observed neurofibrillary tangles are composed of argentaphilic fibers arranged in irregular bundles, knots, and curves.

The senile or neuritic plaques were the most conspicuous histologic lesions observed in sections stained with the Bielschowsky technique.
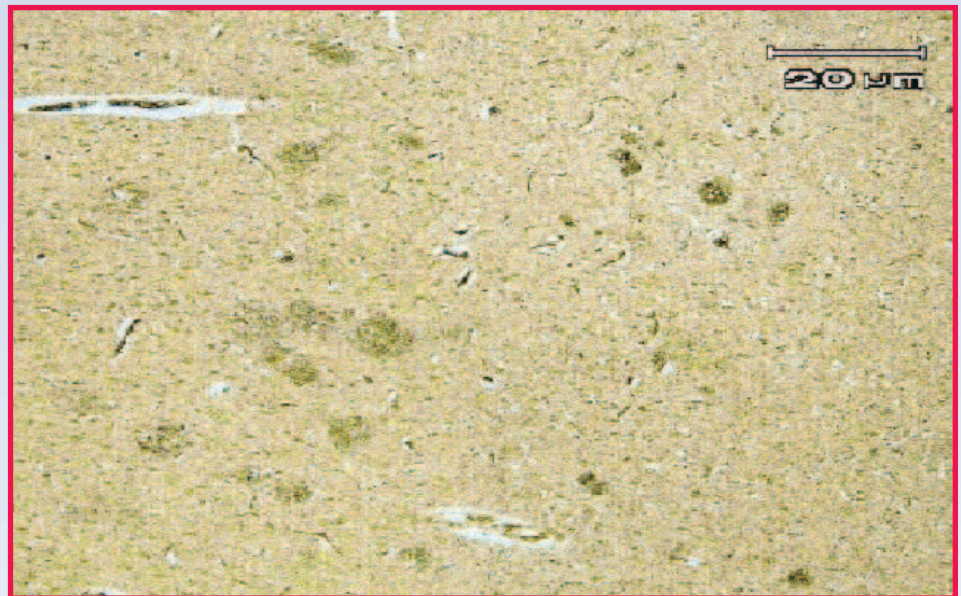

Fig. 5. Section of cortex from a patient with AD, demonstrating senile plaques. Bielschowsky stain, microwave method. 40X
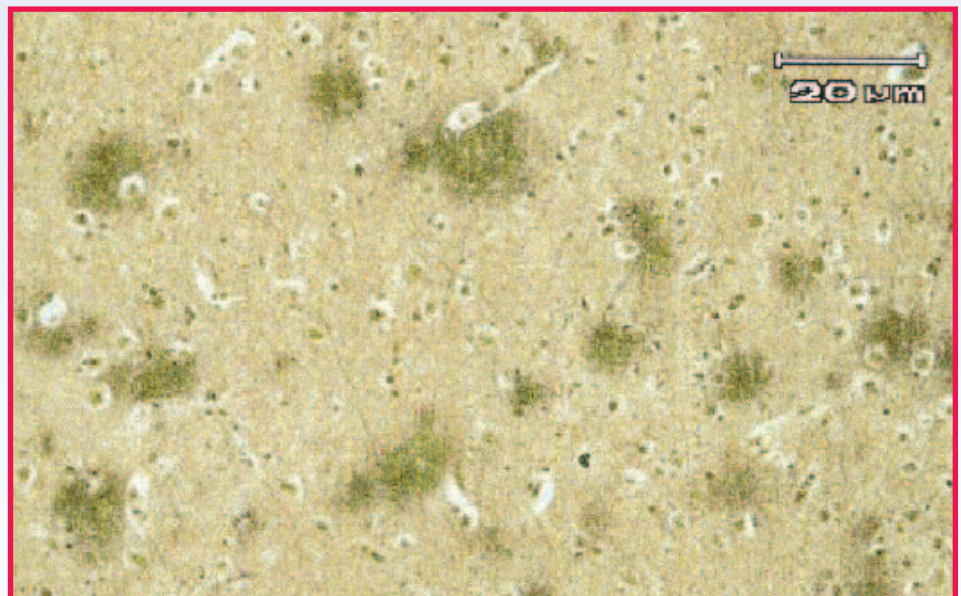

Fig. 6. Section of cortex. Numerous senile plaques are observed. Bielschowsky stain, microwave method. 100X
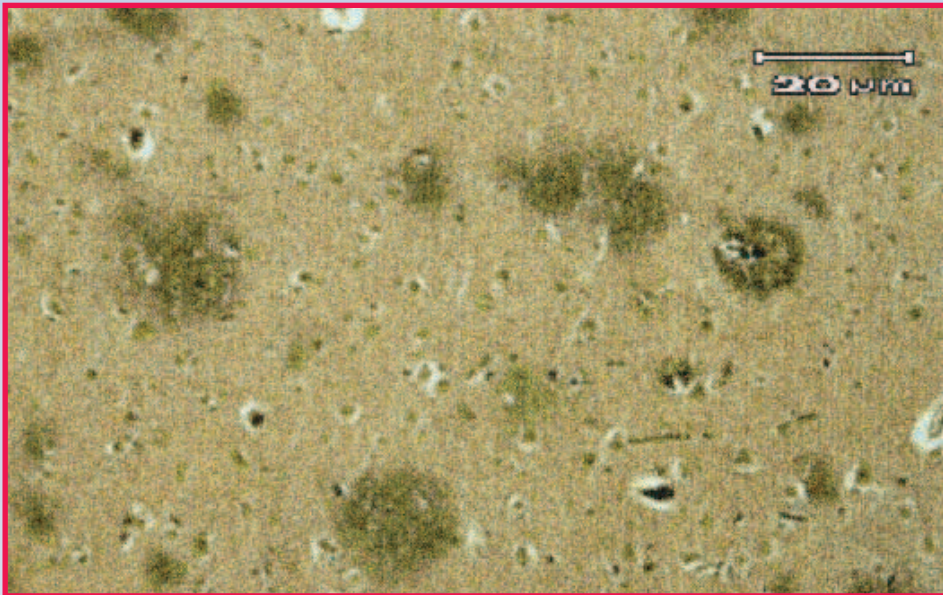
23

Fig. 7. Three different types of neuritic plaques are observed. Diffuse plaques, primitive plaques without a ß-amyloid core, and classic plaques are evident. 100X
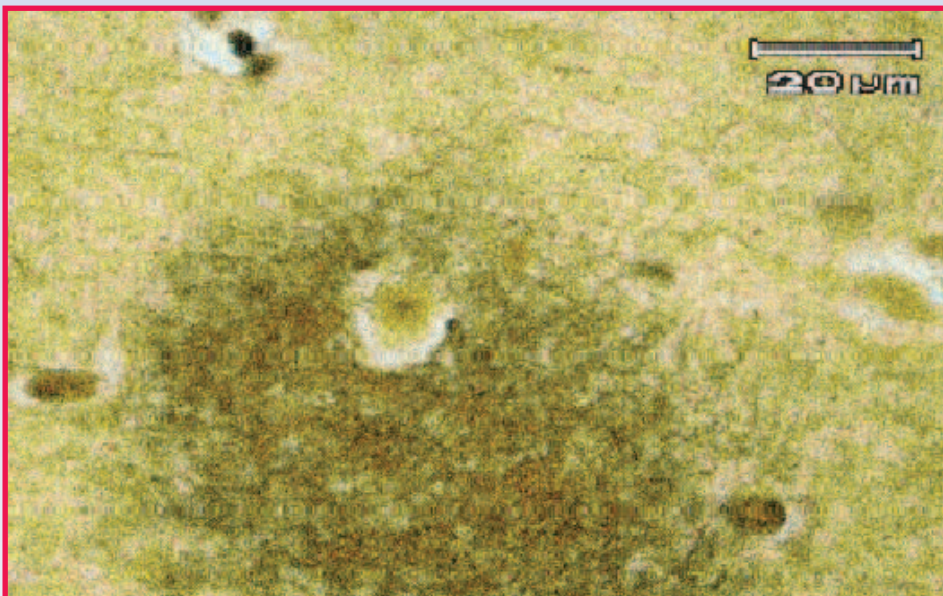

Fig. 8. Senile plaques. Bielschowsky stain, microwave method. 400X

The neuritic plaques (Figs. 3, 5, 8, 9, 10) are patches or flat areas composed of clusters of degenerating nerve terminals arranged around a central core of ß-amyloid peptide (BAP). Neuritic plaques are argentaphilic and contain abundant glial processes as well as deposits that stain positively for amyloid.[4] These plaques were found in areas of the cerebral cortex that are linked to intellectual function. BAP is a fragment of a much larger membrane-spanning amyloid precursor protein (APP). The function of APP is unclear, but it appears to be associated with the cytoskeleton of nerve fibers.[4] Normally, the degradation of APP involves cleavage in the middle of the BAP portion of the molecule, with both fragments being lost in the extracellular fluid. In Alzheimer's disease, the APP molecule is cut at both ends of the BAP segment, thereby releasing an intact BAP molecule that accumulates in neuritic plaques as amyloid fibrils[5] (Fig. 9). The core of these plaques contains a distinct form of BAP, which is 40 amino acids in length. BAP is derived from proteolysis of a much larger (695 amino acids) membrane-spanning amyloid protein.[5] Under the microscope, different developmental stages of neuritic plaques were observed. In Figs. 3A, 5, 6, 7, diffuse plaques are observed; primitive plaques without a ß-amyloid core are observed in Figs. 3A, 6, 7. Classic neuritic plaques are observed at low magnification in Fig. 3B (100X) and at higher magnification in Fig. 10 (400X). In our laboratory, the quantitative studies of different plaques and comparison of staining methods in serial sections are underway, as well as the electron microscopy of such cases.

Discussion

The incidence of the progressive neurological disorder known as Alzheimer's disease is characterized by loss of memory, carelessness about personal appearance, emotional disturbances that progress to complete disorientation, severe deterioration in speech, incontinence, and stereotypical repetitive movements. Pathologic changes include cortical degeneration that is more marked in frontal, temporal, and parietal lobes. Characteristic degeneration includes a decrease in neurons in regions of the brain that are responsible for cognition, memory, and other thought processes. The cause of AD has not been fully elucidated, but there have been significant advances in our understanding of the origin of both AD-associated amyloid in the neuritic plaques and the neurofibrillary tangles in the cytoplasm of neurons.

In our AD cases, paraffin-processed tissue sections of cortex stained with Bielschowsky silver stain have given consistent results. In the future, we plan to do more
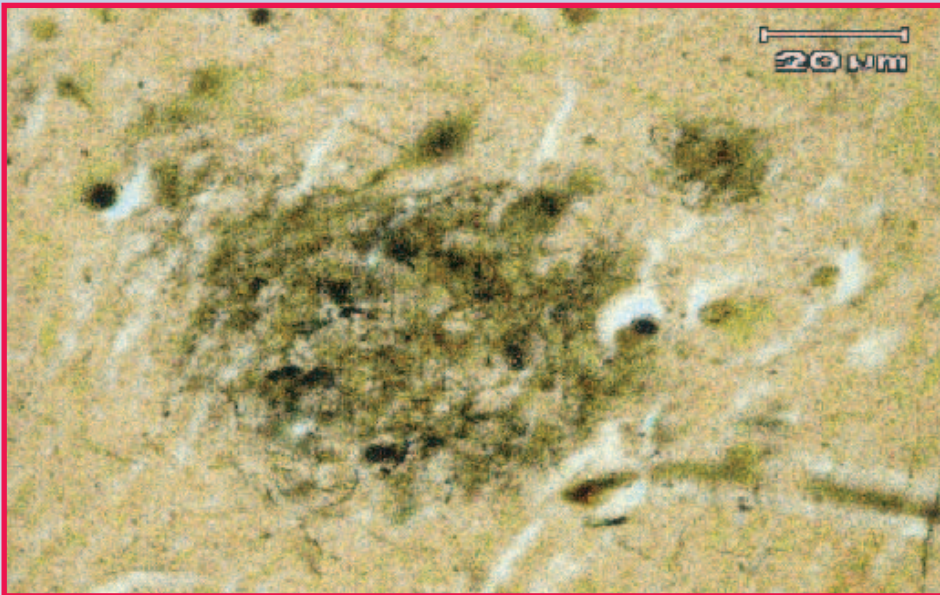
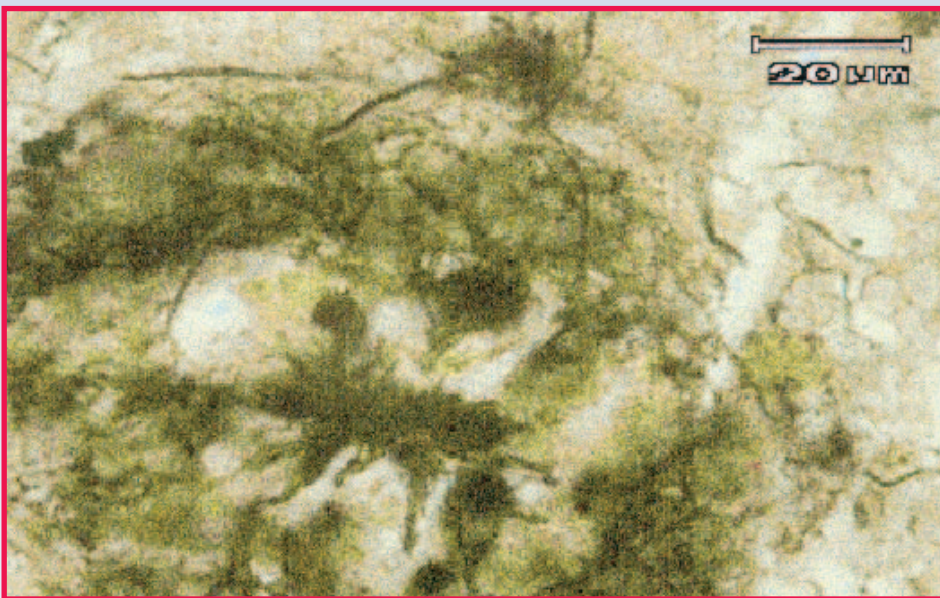Fig. 9. Senile plaque. Bielschowsky stain, microwave method. 400X

Fig. 10. Senile plaque stained with Bielschowsky (microwave method) at 400X. The senile plaque presents an abnormal spherical structure that consists of an amyloid core surrounded by dystrophic neurites, astrocytes, and microglial cells.

quantitative and morphological analysis. Application of the microwave modification to various sections may translate into significant savings in time and resources. The application of this staining technique to AD pathology offers many possibilities for the study and quantification of neuritic plaques, neurofibrillary tangles, and granulocortical degeneration using both light microscopy and transmission electron microscopy.

References

1. Reusche E. Silver staining of senile plaques and neurofibrillary tangles in paraffin sections: a simple and effective method. *Pathol Res Pract*. 1991;187:1045-1049.
2. Bancroft JD, Stevens A, eds. *Theory and Practice of Histological Techniques*. 4th ed. New York, NY: Churchill Livingstone; 1996.
3. Carson FL. *Histotechnology: A Self-Instructional Text*. 2nd ed. Chicago, Ill: American Society of Clinical Pathology; 1997.
4. Navarro A, Tolivia J, del Valle E. Congo red method for demonstrating amyloid in paraffin sections. *J Histotechnol*. 1999;22(4):1-5.
5. Navarro A, Astudillo A, del Valle E, Gonzalez C, Tolivia J. Immunohistochemical presence of apolipoprotein D in senile plaques. *J Histotechnol*. 2001;24(1):45-48.

Combined UCHL-1/PASH Staining in the Diagnosis of Renal Transplant Rejection

Ranjitha Veerappan, MD;
Lou Ellen Miller, HT (ASCP);
Piyush Joshi, MD;
George A. Youngberg, MD
Pathology Department
East Tennessee State University
Johnson City, TN
veerappa@mail.etsu.edu

Introduction

Determining if the cause of renal allograft dysfunction in the early posttransplant period is due to rejection or other reasons is a daunting task for the clinician. Clinical signs and symptoms alone are not helpful in clearly distinguishing the numerous causes of renal dysfunction. Various noninvasive tests including imaging studies have also been unsuccessful in distinguishing rejection from other causes.[1] Renal allograft biopsy has, therefore, emerged as a key element in aiding in the accurate diagnosis of transplant rejection.

An allograft biopsy in the context of acute rejection not only helps to confirm the diagnosis, but it also reveals if the rejection is a result of humoral (antibody-mediated) or cellular immunologic mechanisms. This distinction determines the therapeutic course and the successful reversal of acute rejection. Cellular rejection is the more common type and is typically manifested by a T-lymphocyte attack directed against renal tubules (and occasionally against blood vessels). Microscopically, the early stages are characterized by edema and focal infiltration of the interstitium and peritubular capillaries by lymphocytes. In later stages, plasma cells, monocytes, and macrophages appear along with a more diffuse lymphocytic infiltrate. Invasion of the tubular epithelium by

lymphocytes is a characteristic finding of tubulointerstitial rejection.[2] To standardize diagnoses and avoid false positives, a formal system for interpreting renal allograft biopsies was developed.[3] In this system, the diagnosis of acute cellular tubulointerstitial rejection is based on the finding of tubulitis. The criterion for diagnosing tubulitis is the identification of intraepithelial lymphocytes in the tubules.

The interpretation of tubulitis has traditionally been done using periodic acid-Schiff hematoxylin (PASH) staining, which clearly identifies the tubular basement membranes and, therefore, aids in the accurate assessment of the location of the lymphocytes (inside versus adjacent to the tubule). However, a significant drawback related to the PASH stain is that intraepithelial lymphocytes cannot always be reliably distinguished from tubular epithelial cell nuclei. Additional stains such as leukocyte common antigen (LCA) and a T-cell stain (UCHL-1) that specifically identifies lymphocytes have been used to address this issue. However, these stains again raise the issue of the location of the lymphocytes (inside versus adjacent to the tubule), since the basement membrane cannot be visualized by these methods. The ideal stain, therefore, would be the one that combines the ability of the PASH stain to visualize the basement membrane and also identify the lymphocytes with a specific marker such as LCA or UCHL-1. This method would greatly facilitate and improve the accuracy of diagnosing acute cellular tubulointerstitial rejection. Such a stain has recently been developed[4] and can be produced using the Ventana Benchmark automated immunohistochemistry staining system and the NexES™ special stains instrument.

Case Report

A 32-year-old man with a live unrelated donor renal allograft was noted to have rising creatinine. His immunosuppressive regimen consisted of rapamycin and steroids, with no mycophenolate mofetil or calcineurin inhibitors. The elevated creatinine did not respond to pulse methylprednisolone, so a percutaneous renal biopsy was obtained.

Methods

Routine light microscopic renal biopsy stains, including PASH and hematoxylin and eosin (H&E), were made using standard methods.

A UCHL-1/PASH stain was prepared according to the method of Resch et al,[4] using a Ventana (Ventana, Tucson, AZ) combined automated immunohistochemical (Benchmark™) and histochemical (NexES) stainer. Briefly, the renal core biopsy was received in Carson's fixative, processed overnight, and paraffin embedded. The sections were cut at 3 microns and stained on the Benchmark using the iView™ DAB paraffin detection kit (Ventana, Tucson, AZ)
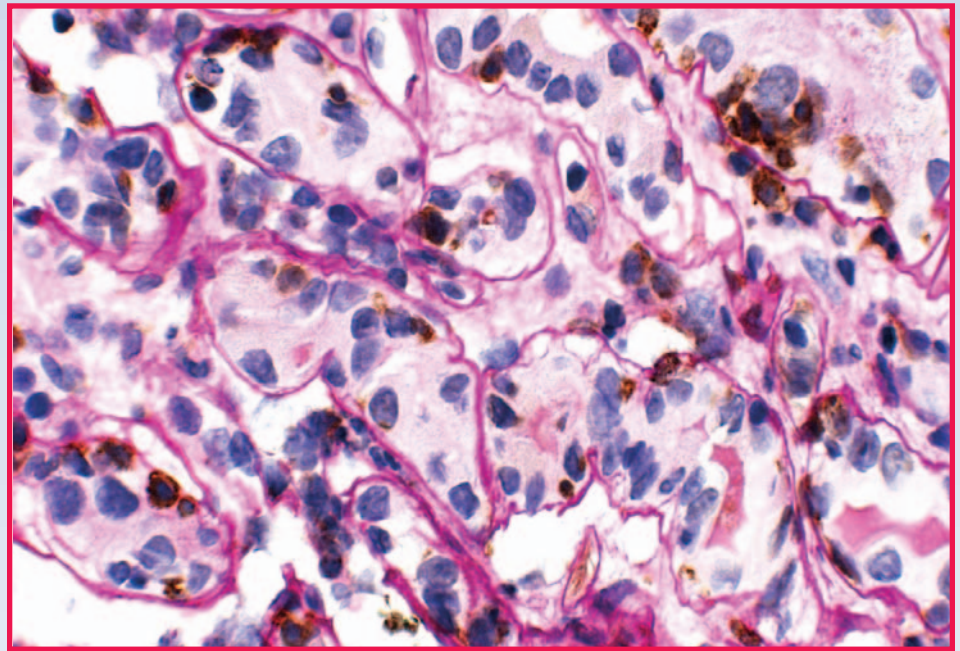

Fig. 1. Tubulitis in the renal biopsy. Lymphocyte cytoplasm stains brown. Tubular borders are clearly delineated. UCHL-1/PASH, 400X
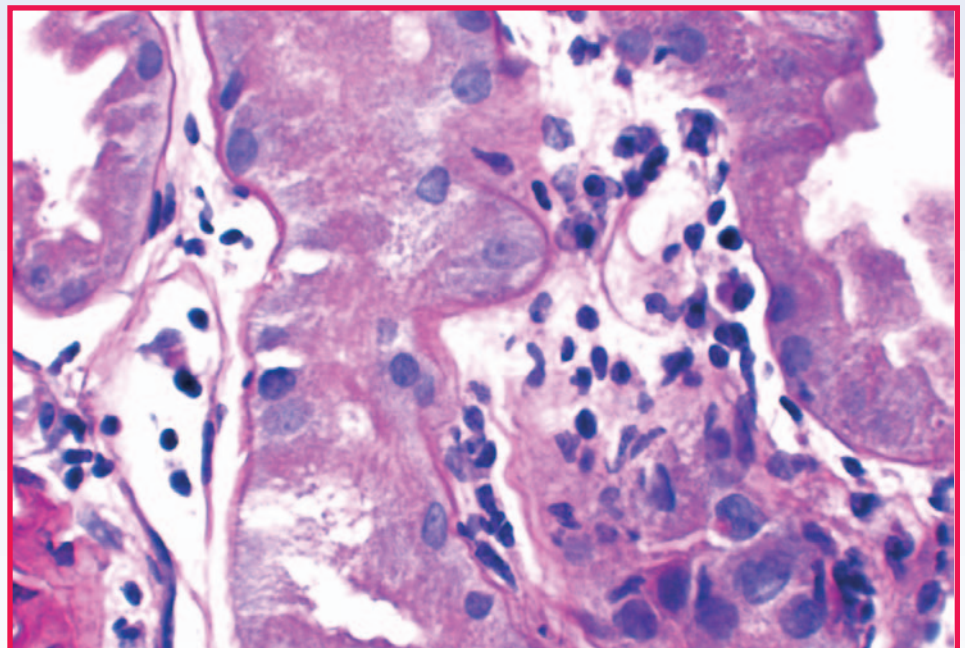

Fig. 2. Distinguishing lymphocytes from tubular cells can be difficult on a standard PASH stain. PASH, 400X

with the T-cell (CD45RO) antibody. After the antibody step, the slides were removed from the Benchmark, rinsed in DI water/Dawn® dishwashing liquid, and placed on the NexES for routine PASH stain. The slides were then dehydrated through graded alcohols, cleared in xylene, and mounted with a permanent mounting medium.

Results

The biopsy demonstrated moderate interstitial inflammation involving greater than 25% of the cortical area. The inflammatory infiltrate consisted predominantly of lymphocytes, with some admixture of plasma cells, eosinophils, and neutrophils. Several tubular profiles showed more than four mononuclear cells per tubular cross-section. This was most clearly demonstrated on the PASH/T-cell stain (Fig. 1). No tubular cross-sections contained more than ten mononuclear cells. The PASH/T-cell stain confirmed that the majority of lymphocytes present were T-cells. A diagnosis of acute cellular rejection, tubulointerstitial type was made (Banff 1997 acute rejection, type IA).

Discussion

The key element in making a diagnosis of acute cellular rejection, tubulointerstitial type, is the identification of tubulitis. This can be challenging because lymphocytes in foci of presumptive tubulitis can be difficult to distinguish from tubular nuclei on standard stains like H&E or PASH (Fig. 2). Immunohistochemical stains for LCA or T-cell markers can reliably identify the lymphocytes, but it may be difficult for these stains to distinguish whether the lymphocytes are truly inside the tubular basement membrane or merely adjacent to the tubule (Fig. 3). Combining a basement membrane stain (PAS) with a T-cell stain (UCHL-1) elegantly solves the problem of both specifically identifying
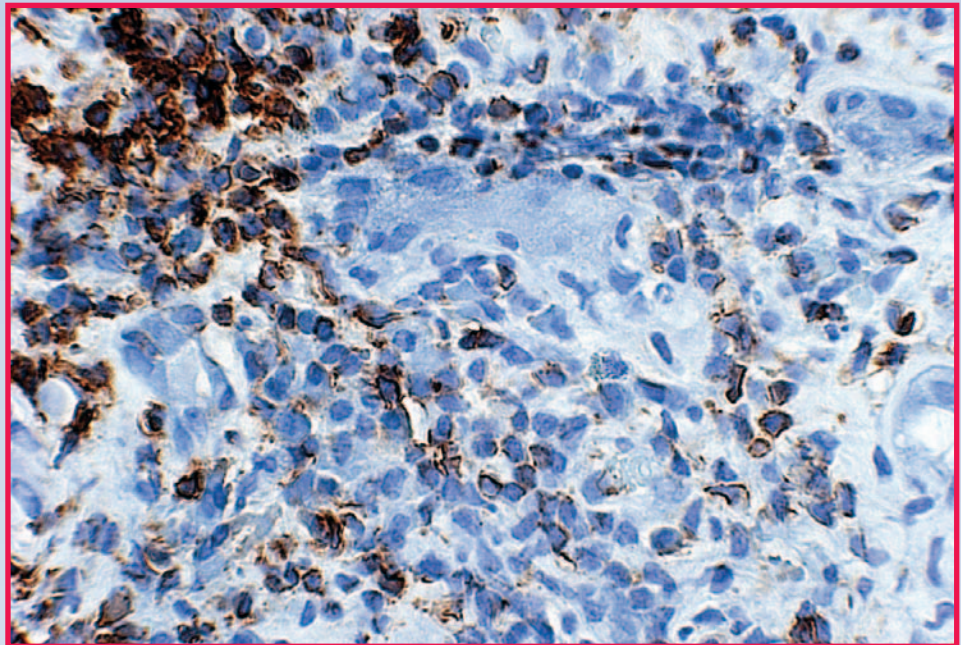

Fig. 3. It is difficult to identify borders of tubules on a standard lymphocyte stain; determining the location of the lymphocytes (outside versus inside the tubular basement membranes) can be problematic. LCA, 400X
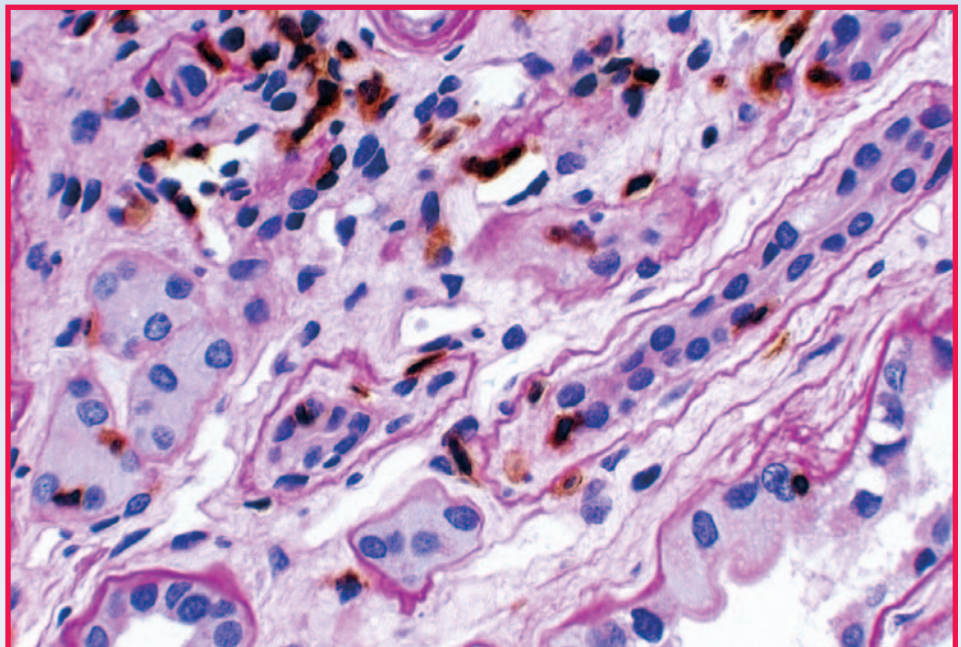

Fig. 4. Lymphocytes are clearly identified, and their precise location in relation to tubular basement membranes is easy to determine on the PASH/T-cell stain. UCHL-1/PASH, 400X

T-lymphocytes and precisely determining their location (Fig. 4). Thus, the presence of tubulitis can quickly and accurately be confirmed or excluded. This combination of UCHL-1/PASH greatly improves the accuracy of diagnosing acute cellular tubulointerstitial rejection and helps determine the therapeutic course and prognosis.

References

1. Brown ED, Chen MY, Wolfman NT, Ott DJ, Watson NE Jr. Complications of renal transplantation: evaluation with US and radionuclide imaging. *Radiographics.* 2000;20(3):607-622.
2. Rosai J. *Rosai and Ackerman's Surgical Pathology.* 8th ed. Elsevier Science; 1996:1115-1116.
3. Racusen LC, Solez K, Colvin RB, et al. The Banff 97 working classification of renal allograft pathology. *Kidney Int.* 1999;55(2):713-723.
4. Resch L, Yu W, Fraser RB, et al. T-cell/periodic acid-Schiff stain: a useful tool in the evaluation of tubulointerstitial infiltrates as a component of renal allograft rejection. *Ann Diagn Pathol.* 2002;6(2):122-124.
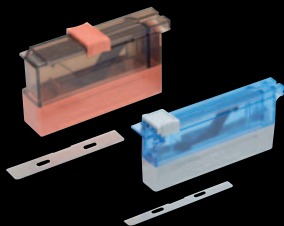
Cryomicrotomy of Murine Tissues for Research Immunohistochemistry and Routine Hematoxylin and Eosin Staining Part II

Gayle M. Callis, MT, HT, HTL(ASCP)
Veterinary Molecular Biology
Montana State University, Bozeman, MT
gcallis@montana.edu

Introduction

Cryomicrotomy Part II is a continuation of "Preparation and Snap Freezing Part I" that appeared in the May 2004 issue of *HistoLogic*.[1] The terms cryomicrotomy and cryotomy are synonyms and will be used interchangeably in this article. Although the techniques presented can be applied to clinical situations, this discussion is directed primarily toward research laboratories working with rodents and other animal tissues. A major complaint by researchers is that frozen sections (FS) have very poor morphology when compared to either paraformaldehyde (PFA) or neutral buffered formalin (NBF) fixed paraffin tissues. However, our laboratory encountered major problems using these aldehyde fixatives for murine lymphocyte (CD) marker immunohistochemistry (IHC) and immunofluorescent (IFA) staining. Unfortunately, and as others have discovered, some murine CD antigens are so compromised by aldehyde cross-linkage that attempts at heat induced epitope retrieval (HIER) or enzyme digestion fail to recover antigenicity, and yield no IHC or IFA staining. Fluorescence and confocal laser scanning microscopy (CLSM) are also plagued with increased autofluorescence as a result of aldehyde fixation.[2] Consequently, cryotomy and organic solvent fixation became our major options to avoid aldehyde fixatives for successful IHC and IFA. We noticed our tissue morphology was very good after acetone/alcohol fixation and somewhat less so after acetone fixation. With organic solvent fixatives, we have excellent IHC and IFA staining and never have to use antigen recovery methods.

Frozen sections may be obtained from either fresh frozen tissues or tissues previously fixed in PFA or paraformaldehyde-lysine-periodate (PLP).[3] Fixed tissues must be cryoprotected in 30% sucrose overnight at 4°C. Tissue collection and snap freezing methods were discussed at length previously.[1] As a reminder, our research tissues are **never** frozen inside a cryostat using a Peltier cooling device or heat extractor. Cryostat freezing temperatures are warmer than the snap freezing temperatures discussed in Part I. Consequently, cryostat tissue freezing is slower and creates large, damaging ice crystal formations, known as freezing artifact, in tissue spaces (Fig. 1). Hematoxylin and eosin (H&E) and other special stains (oil red O for lipids) can be done with FS, in addition to IHC/IFA methods. This article will discuss general cryostat setup and usage, ergonomics, cryostat chamber temperature differentials, optimal sectioning temperatures for different tissues, microtome blades, hints on specimen block orientation, cryosectioning, biohazards, as well as block and FS handling and storage.

Cryostat

A primary consideration is which cryostat is best suited for research cryomicrotomy. With so many choices, any cryostat available should work well. Cryostats come with either manual or motorized operation, and the latter is becoming more popular because it helps in preventing repetitive motion injuries. Our cryostats need little space, are easy to defrost and clean, are ergonomically comfortable to use, and have excellent, uncrowded chamber space to work in and to hold multiple blocks. A tall, comfortable chair with a pneumatic lever permits seat height adjustment to accommodate tall and short technicians. During cryostat operation, technicians should sit rather than stand to help prevent stress on back, arms, and neck. Jars of stain or fixative should not be
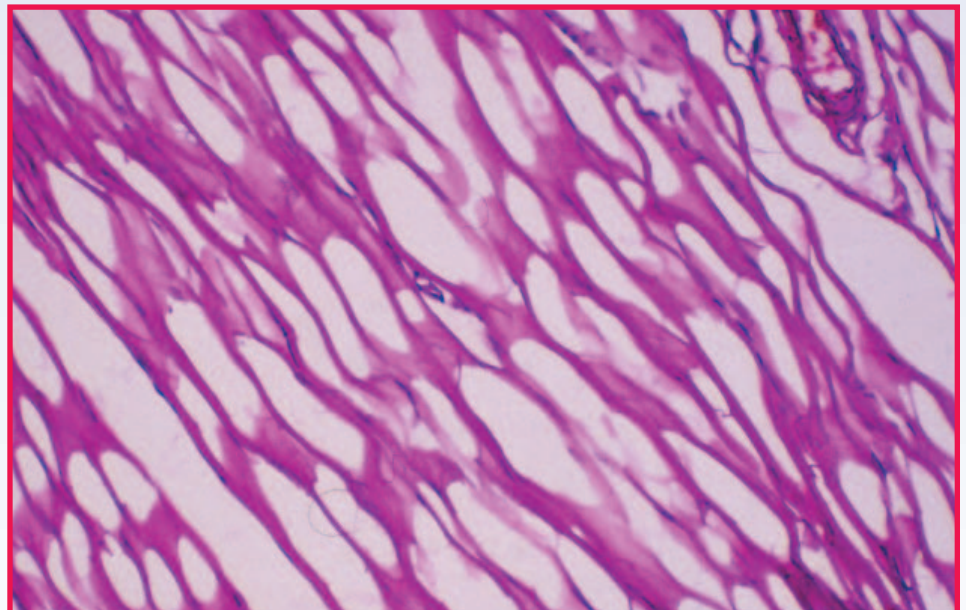

Fig. 1. Freezing artifact in muscle shows severely damaged morphology by water ice crystal formation. Muscle is no longer recognizable. NBF-fixed frozen section, H&E. 40X

placed on top of cryostat or inside the chamber in order to prevent spills in a chamber or on electronic components of the instrument. A counter or cart placed next to a cryostat provides an extra work area within easy reach of the operator. Our laboratory has one cryostat designated for Biosafety Level 2 prion tissues, and it is kept in a separate room.

Cryostat Chamber and Temperature Differentials

Cryostats have warm and cold areas within the chamber, and these areas can be used to make cryosectioning less difficult. Our cryostats have metal bars with holes to hold metal disks (or tissue chucks) and a Peltier cooling plate. These bars keep blocks 10°C *colder* than the programmed temperature of the instrument cabinet. Mounting blocks using cold bars or a Peltier device can cool blocks in excess of -30°C to -40°C. These colder temperatures can make some tissues too cold for immediate sectioning. After using a thermometer to find our cryostat chamber's warm/cold spots, we learned that areas immediately adjacent to the microtome were the same temperature as the chamber temperature at the microtome block and knife holders. Newly mounted, colder blocks are placed next to the microtome to equilibrate to a desired sectioning temperature for 20 minutes before cryotomy. We can store up to 20 mounted blocks in a handy plastic microcentrifuge tube rack next to the microtome to keep the blocks ready for sectioning at the desired temperature. Immediate sectioning of -30°C to -40°C blocks resulted in shattered, ugly liver, brain, and spleen frozen sections. One must be aware of the cryostat's cooling capabilities, temperature differentials, and how these conditions can be optimized to get a good frozen section.

Mounting Blocks Onto Metal Chucks

Tissue-Tek® O.C.T. Compound (Sakura Finetek, Torrance, CA)

embedded blocks removed from a -80°C freezer must be placed in the cryostat chamber to allow them to equilibrate to sectioning temperature. This takes approximately 20 to 30 minutes. To speed up our temperature equilibration, we now mount -80°C blocks immediately after removal from the freezer. The key is to wait for the tissue to be at the required sectioning temperature. Large blocks are mounted on large block holders to ensure good support under the whole block. We purchased additional mushroom-style chucks with waffle-weave tops and shortened the stems so the back of the disk fits flat against the microtome. A generous drop of OCT is applied under the block to provide firm support and avoid overhanging edges. Bubbles trapped *under* the block lead to chatter, "chopped" blocks with lost tissue, or block separation during sectioning. Bubbles can be avoided by pushing the block *firmly into the OCT* using another cold disk. Mineralized bone blocks are mounted on waffle-weave chucks using 2% methyl-cellulose, water soluble (Aldrich Chemical Co., Milwaukee, WI). Frozen methylcellulose is *extremely* hard for extra holding power and

vibration-free frozen bone sectioning.

Cryosectioning Temperatures

Technicians should test cryosectioning temperatures for any given tissue using their chosen cryostat. Because tissues have different sectioning qualities, densities, and homogeneity (liver, spleen, brain), we select a sectioning temperature best suited to cut a good FS from the tissue. Cryosectioning brain, liver, spleen, fatty tissue, and bone can be very difficult if the tissue and blade temperatures are not optimal and identical. After trial and error, we found temperature settings and guidelines that worked best for us (Fig. 2). *One must be **willing to change the temperature** in order to obtain a good frozen section.* Mineralized bone is routinely cryosectioned using CryoJane® Tape-Transfer System (Instrumedics, Hackensack, NJ). Acid decalcified bone must be thoroughly rinsed in running tap water followed by 30% sucrose cryoprotection. Residual acid in unwashed decalcified bone trimmings could corrode metal cryostat parts. EDTA-decalcified

Suggested Cryosectioning Temperatures for Tissues	
Tissue	**Cryosectioning Temperature of Blade and Tissue**
Normal or inflamed tissues; lymph nodes, small intestine, Peyer's patches, kidney, and stomach	-20°C
Spleen, liver, brain, spinal cord Brain, prefixed/sucrose cryoprotected for thick 50 μm sections	-17°C to -16°C -19°C or warmer
Skin folded into "V" shape with hair oriented inside the "V"	-20°C
Mineralized bone Extremely fatty tissue, oily mink skin	-28°C to -32°C with CryoJane
Lung—fresh, unfixed, OCT-filled Lung—fresh, *not* OCT-filled Lung and mouse nasal turbinates—PFA- or PLP-fixed with 30% sucrose cryoprotection	-20°C -26°C with CryoJane -26°C prevents sucrose *oozing out of frozen tissue block*

Fig. 2. Temperature settings used in our lab. *Cryosectioning temperature settings may vary depending on the cryostat.*

and sucrose-cryoprotected mouse nasal turbinates are easily sectioned using high-profile disposable blades.

Microtome Blades

Our laboratory prefers Accu-Edge® (Sakura Finetek, Torrance, CA) high-profile (over low-profile) disposable blades. We found no difference in sharpness between high- or low-profile blades, but wider, thicker high-profile blades proved more stable during cryotomy. However, technicians should choose the optimal blade for their needs. The blade is moved frequently to ensure the sharpest edge; care is taken to avoid damaging the edge with a brush or gauze. The blade holder must be cleaned, lubricated, and properly adjusted, with no loose screws or levers. Angle settings can be changed by an accidental loosening of the adjusting levers or unfamiliarity with knife holder operation. A desired blade angle setting can be marked using a Sharpie® marker on top and bottom of the knife holder for a quick realignment of a "lost" angle setting. A used blade should not be returned to the package slot *but disposed of in a biohazard sharps container*. Mineralized bone can be sectioned with either a D or C profile *tungsten carbide* (TC) tipped, steel back cryostat knife (Delaware Diamond Knives, Wilmington, DE). Tungsten carbide blades are expensive and must be kept extremely sharp and in prime condition for bone cryotomy. Steel blades, C profile, work well for all tissues except bone and must be free of nicks or rust, and sharpened frequently with a good knife sharpener or reconditioning service. A dull blade of any design will be useless for cutting good frozen sections.

Cryomicrotomy
Block Orientation

The block and/or tissue is oriented in the microtome holder to provide a path of least resistance during sectioning. Rather than place a block with the long edge of tissue
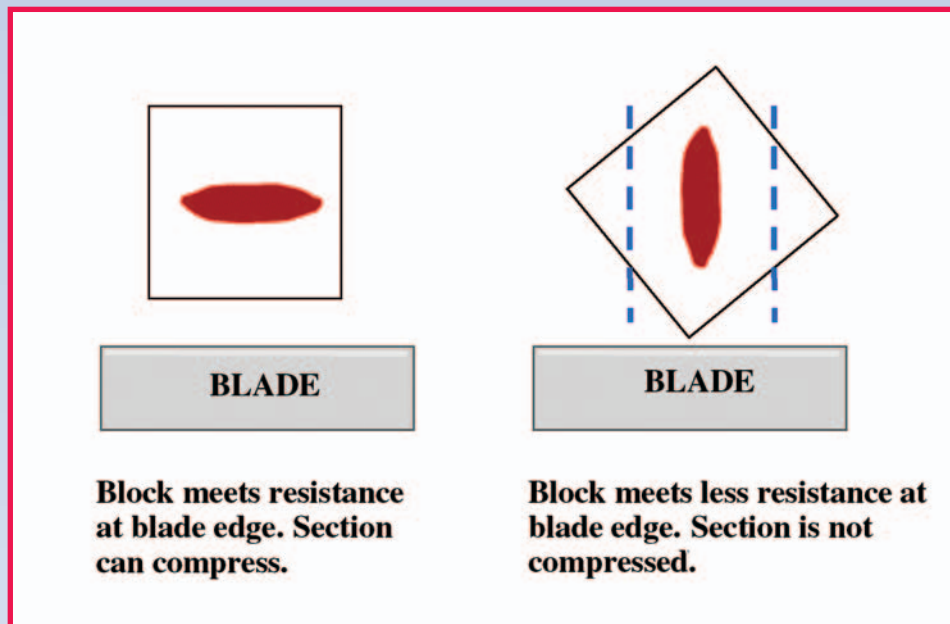

Fig. 3. Block with mouse spleen. Block face oriented to blade edge for resistance-free cryotomy and uncompressed spleen FS. Blue dotted line indicates where OCT is trimmed away using room temperature, Teflon®-coated razor blade. This shapes the block and removes excess OCT, if needed.
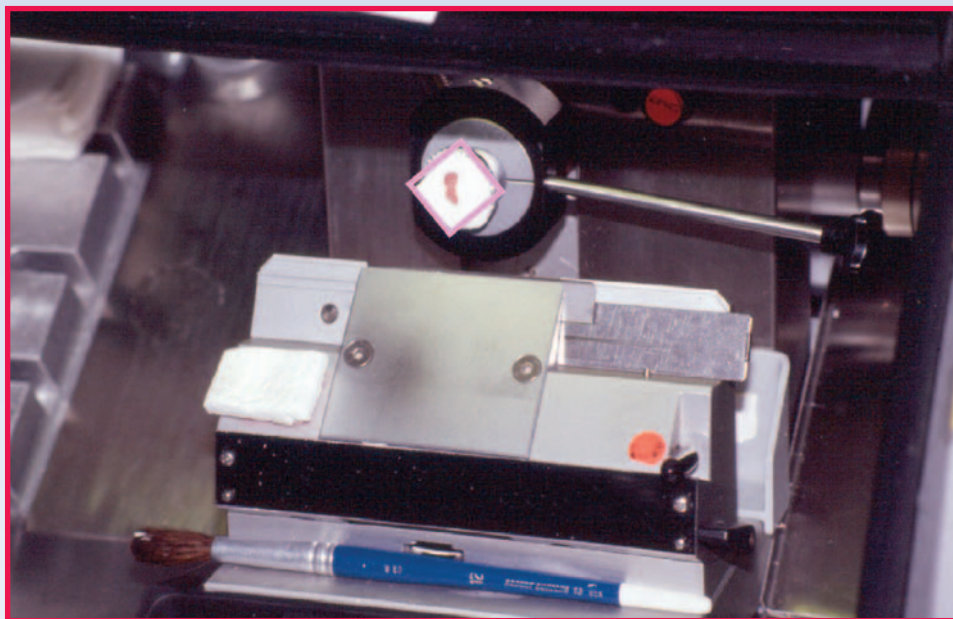

Fig. 4. Mouse spleen in block oriented as a (pink) diamond for *"path of least resistance"* cryotomy. Styrofoam finger rest is seen on left side of blade holder. Anti-roll plate is removed for brush technique sectioning. Trimmings are pushed behind blade with large blue cleaning brush.

parallel to the blade edge, we turn the block so it looks like a diamond with one corner pointed down toward the blade edge (Figs. 3, 4). This allows the block and tissue to contact the edge *en pointe* with less resistance as the tissue begins to section. One can actually feel this resistance during a sectioning stroke as block and tissue meet the blade. Initial tissue orientation *at embedding* is also important to enable cryotomy. [2]

Cryosectioning

Proper safety precautions must be taken for known or potentially biohazardous agents. A dedicated cryostat or special biosafety containment area may be necessary when working with infectious bacteria, viruses, and prions in tissue. Gloves have not hindered cryosectioning techniques or manipulation requiring fine dexterity. Reusable silk glove liners (www.wintersilks.com) may be

worn inside disposable gloves to keep hands warm and dry during long cutting sessions.

Cryotomy is very easy to learn with patience and practice. How others perform this task varies greatly; this led to a lively demonstration and discussion at a hands-on workshop at the 2003 NSH.[4] We prefer to remove or not use the anti-roll plate in favor of the cold "brush technique." As a 5 μm FS begins to pass over the blade edge, a fine camel's hair brush is used to capture the curl, and the section is gently *guided but not brushed* onto the blade holder (Fig. 5). The brush technique is very fast, does not prevent serial sectioning, and avoids the need for repeated cleaning and adjustment of the anti-roll plate. A styrofoam square taped onto the blade holder allows the technician to rest the little finger for a relaxed hold on the brush; it also aids in frostbite prevention (Fig. 4). The anti-roll plate is reinstalled to keep thick, 50 μm brain sections from curling over, as thick section manipulation is harder to control with a brush.

The cryostat flywheel should be turned *slowly and continuously so the blade passes through the tissue smoothly*. Hesitation during flywheel rotation creates a jerky motion and the tissue section will have uneven thick/thin areas. A light grip of the flywheel handle works best. A FS can be picked up two ways from the blade holder. With the first method, a room temperature slide is lowered with a quick, featherlight motion toward, and then away from, the FS to attract (also known as flash dry) the section onto the slide. The section must never be pushed against the holder by a slide or the FS will melt and refreeze *onto the holder*. The other method requires that slides be cooled inside the cryostat. After a FS is cut, it is manipulated, using the brush, from the holder onto the top of a cold slide. The section will adhere to the slide by warming the back of the slide with your hand or finger.
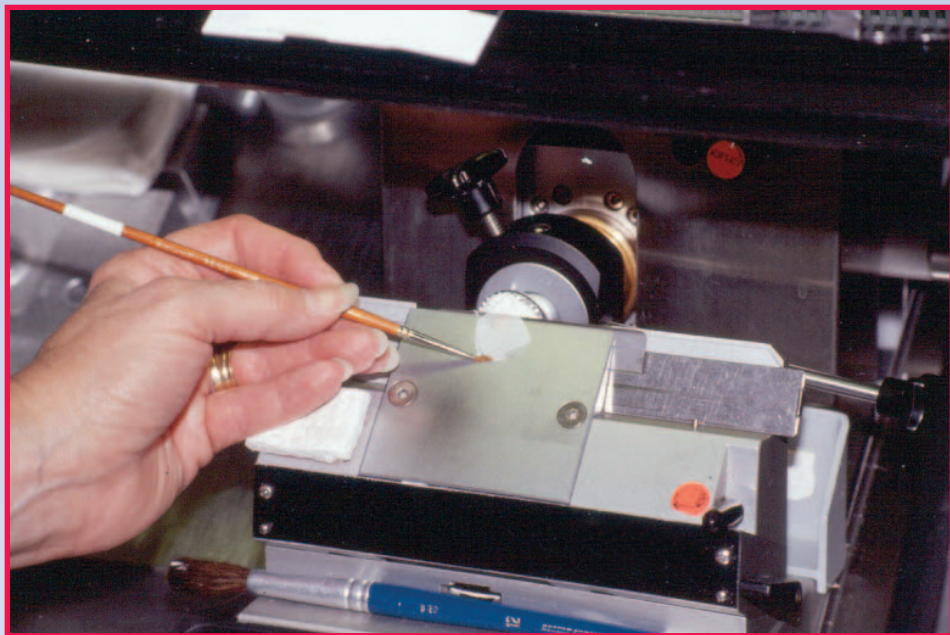

Fig. 5. Brush technique used to guide section onto blade holder before pickup onto a glass slide, while block stays down and behind the blade. Note side of finger resting on styrofoam for relaxed brush control.

Block Storage
After sectioning, blocks are sealed with a *thin* OCT layer smeared across the block face and allowed to freeze. Sealed blocks help prevent tissue from drying out during freezer storage. Large drops of OCT on top of tissue are avoided to prevent melting and refreezing of tissue. One should be able to recut a sealed block and not lose valuable tissue to excessive retrimming. *Never store frozen blocks in a cryostat chamber or self-defrosting freezer.* Defrost cycles can cause freeze/thaw damage to antigens and create freezing artifact in tissue. Sealed blocks can be wrapped with aluminum foil, marked with a Sharpie marker, put into ziplock bags or 50 ml screw top centrifuge tubes, and stored in a -80°C freezer for a period of years, or a -27°C freezer for a period of months. We have been able to resection tissue after 6 years of storage at -80°C while retaining excellent morphology, antigenicity, and sectioning quality.

Cryostat decontamination remains controversial as some products have a high water content (Clorox®), which causes ice buildup, some are corrosive to cryostat parts, and others allow for toxic fume exposure (formalin). Some cryostat manufacturers tout decontamination features, but these may not work for infectious agents resistant to heat, formalin, or low Clorox concentration.

Frozen Section Handling and Storage
Frozen sections on slides destined for IHC/IFA *should not be stored in a cryostat immediately after sectioning*. When a FS is moved from the cryostat to room temperature, water condensation forms on top of the FS. This condensation can cause damage to tissue morphology. An exception is FS for laser capture microdissection (LCM) and in situ hybridization (ISH) work.[4] After slide mounting, these FS are kept on dry ice (approximately -90°C) or in a black slide box surrounded by dry ice inside the cryostat to minimize RNA loss.

How a FS should be stored depends on what ultimately will be done to the section. For an H&E stain, a fresh, unfixed FS can be immersed immediately into room temperature NBF or PFA, fixed for 10 minutes or more, rinsed with distilled water, and stained with a routine H&E method. We found
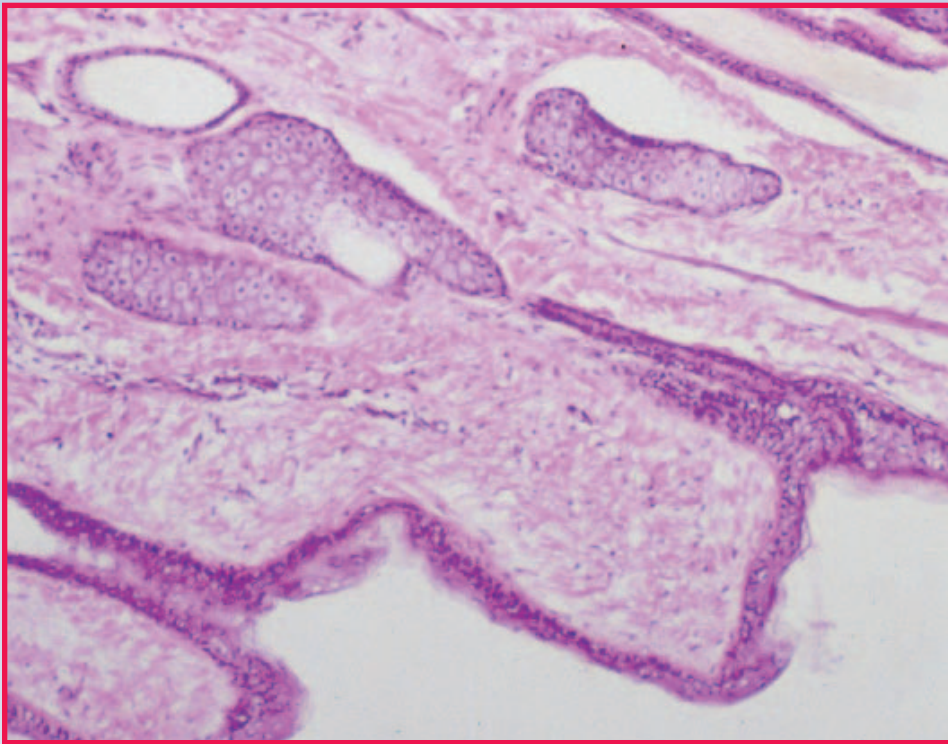
Fig. 6. Fresh bovine skin, 5 μm FS, NBF fixed, then stained with H&E. 20X

that these H&E stained FS had good morphology preservation comparable to paraffin-embedded tissues (Fig. 6).

Frozen Sections for IHC/IFA Procedures

In our lab, antigen stability dictates FS storage conditions, e.g., temperature and time. Our perfused fixed tissue (PFA or PLP) FS are air dried at RT for 30 minutes (minimum) and placed into either a black slide box (25 slots) or 5-slide mailer(s) inside a ziplock bag. Nylon bags filled with 16 mesh silica gel were placed into storage containers to maintain dry conditions. Freezer storage can be at -80°C (for several weeks) or sometimes at -27°C (for up to a week), with -80°C the preference. Before IHC staining, the slide box is removed from the freezer and *not opened for 30 minutes* to allow the sections to equilibrate to room temperature. Boxes are never to be opened to take out just a few slides and then reclosed and returned to the freezer. Freeze/thawing of sections and water condensation must be avoided to prevent loss of antigenicity. These freezer storage conditions and the temperature

equilibration are done with *all* our unfixed and fixed frozen sections.

Fresh unfixed frozen sections are handled in 4 ways. It is recommended that optimal fixation parameters (length of air drying, type of fixative, fixation time, and temperature) be determined for your laboratory's IHC/IFA staining success.

1. Fresh tissue FS are air dried for 30 minutes (minimum) and stored unfixed using previously described freezer storage procedures. *On the day before we perform IHC,* stored sections are removed from -80°C and *allowed to air dry at RT overnight inside the closed box.* These FS are fixed just before beginning the IHC protocols.

2. Fresh tissue FS are air dried 30 minutes to several hours, then fixed in 4°C acetone, air dried to disperse acetone fumes, then stored as described. Acetone-fixed sections are removed from the freezer *on the day of staining* using described temperature equilibration of sections in the closed slide box.

3. Fresh tissue FS are air dried overnight at RT. Dry FS are fixed in *either* RT 75% acetone in absolute ethanol (5 min) and buffer rinsed, *or* 4°C acetone (10 min), air dried and buffer rinsed, followed by IHC staining. These are the preferred fixation methods in our lab.

4. In one day, fresh tissue FS are cut, air dried for 30 minutes (minimum), fixed with a 4°C acetone method, and IHC stained.

Summary

Frozen sections, although not always popular, are often what researchers must accept in order to obtain good immunostaining results. Our laboratory now performs more cryotomy than paraffin microtomy, and we enjoy excellent tissue morphology and IHC staining results. On a personal note, I actually prefer doing cryotomy to paraffin work. The cryosectioning technique is easy to learn and teach to others. By cleverly using a cryostat chamber's warm and cold spots and choosing a sectioning temperature suitable for a tissue, cryotomy can be efficient and trouble free. Without exception, a blade edge must be sharp and free of nicks. With proper snap freezing, careful cryosectioning, block and section handling, fixation, and staining, the sometimes dreaded FS can be highly acceptable. For those who have done paraffin sections exclusively and suddenly have to do cryomicrotomy, be patient, pay attention to fine detail, relax, and enjoy the challenge of getting the perfect frozen section.

References

1. Callis G. Preparation and snap freezing of murine tissues for research immunohistochemistry and routine hematoxylin and eosin staining. *HistoLogic.* 2004;37(1):4-7.

2. Billinton N, Knight AW. Seeing the wood through the trees: a review of techniques for distinguishing green fluorescent protein from endogenous autofluorescence. *Anal Biochem.* 2001;291:175-197.

3. McLean IW, Nakane PK. Periodate-lysine-paraformaldehyde fixative: a new fixation for immunoelectron microscopy. *J Histochem Cytochem.* 1974;22:1077-1083.

4. Callis G, Sterchi DL. Cryomicrotomy for research murine immunohistochemistry and laser capture microdissection. National Society for Histotechnology S/C. Louisville, Ky; 2003. Workshop #3.

Alcian Blue-H&E-Metanil Yellow Stain for Diagnosing Barrett's Esophagus

Wendi Edgett, BS, HTL(ASCP)
Genesys Regional Medical Center
Health Park Campus
Grand Blanc, MI
wedgett@yahoo.com

Introduction

Barrett's esophagus is a condition that can lead to adenocarcinoma. Proper diagnosis and follow-up treatment is very important for patients diagnosed with this disorder. Sometimes it can be difficult to diagnose. The Alcian Blue-H&E-Metanil Yellow (AB-H&E-MY) stain is very effective in distinguishing between Barrett's and other gastrointestinal disorders. It is simple to perform, and the results can be easily duplicated from one staining batch to another. This stain helps save time and money by combining multiple stains to demonstrate many structures.

Discussion

The gastrointestinal (GI) tract is composed of four distinct layers: the mucosa, submucosa, muscularis propia, and adventitia. The epithelium of the GI tract varies distinctly as you transition from one area of the tract to the next, from the esophagus through the stomach and the intestine. The epithelium is very specific to the properties and purpose of each area of the tract. The esophagus is composed of stratified squamous epithelium that provides protection from contact with the food we swallow (Fig. 1). The point in which the esophagus and the stomach meet is called the gastro-esophageal (GE) junction, where there is a distinct change from the stratified squamous epithelium of the esophagus to the absorptive tubular epithelium of the stomach (Fig. 2). The epithelium of the stomach has mucus-secreting glands that contain neutral mucins.
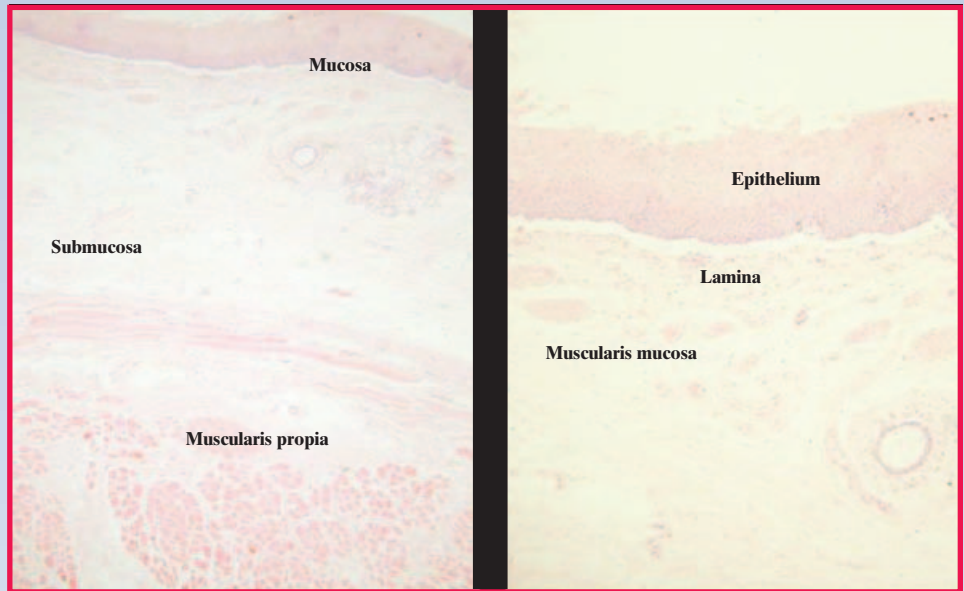
Fig. 1A. GI tract layers. H&E; 10X

Fig. 1B. Esophageal mucosa. H&E; 40X
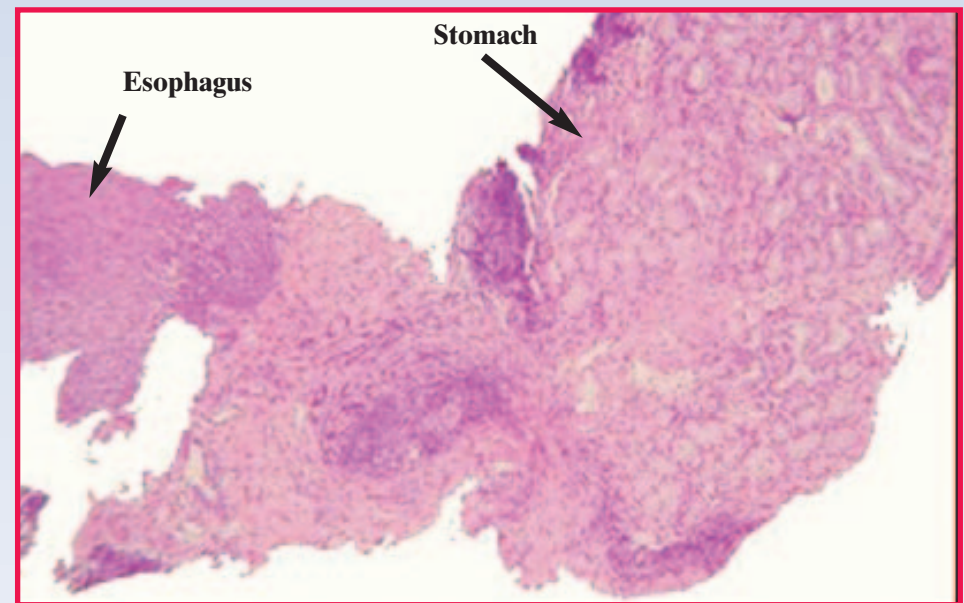
Fig. 2. Gastroesophageal (GE) junction. H&E; 40X

The intestine is composed of tubular epithelium that contains mucin-secreting goblet cells.[1]

Barrett's esophagus is a condition that occurs when the normal squamous epithelium of the esophagus is replaced by intestinal columnar epithelium. This arises from the chronic irritation caused by gastroesophageal reflux disease (GERD). Acid from the stomach causes the cells of the esophagus to be damaged. When they are regenerated, they may be replaced with the columnar epithelium similar to that found in the intestine. This is called metaplasia. An individual with the presence of intestinal metaplasia will be monitored with repeat biopsies approximately every 2 years if no dysplasia is found and every 6 months if dysplasia is present.[2-5]

Endoscopic biopsies comprise a large percentage of the specimens we process in the lab, and among these biopsies, a large number are esophageal biopsies. These biopsies are generally very small fragments of tissue that routinely are cut with two or three levels per block. By picking up a section from each level

for the special stain at the same time that the sections for hematoxylin and eosin (H&E) staining are cut, it gives the pathologist the opportunity to evaluate both slides at the same time.

H&E, the most frequently used stain in histology labs, stains a vast array of tissue structures, providing a simple and comprehensive starting point for the pathologist to make a diagnosis. The hematoxylin is used to stain the nuclear chromatin, which renders the nuclei blue. The eosin is used to stain the connective tissue, whose components appear in three shades of pink—red blood cells stain the darkest, muscle stains slightly lighter, and collagen stains the lightest shade of pink.

The alcian blue stain is primarily used to stain for acid mucopolysaccharides. At a pH of 2.5 it will stain both sulfated (sulphomucins) and carboxylated (sialomucins) mucopolysaccharides, which are found in the goblet cells in the intestine. The alcian blue dye is a very large, positively charged molecule in solution that will bind to the negatively charged low density mucin found in the goblet cells, staining them blue.[6] The alcian blue can be modified to distinguish between the acid mucins by modifying the pH of the staining solution. In the AB-H&E-MY stain, alcian blue is used at a pH of 2.5. The gastric mucosa of the stomach is composed of mucus-secreting cells. These cells contain neutral mucopolysaccharides and typically do not stain with alcian blue; however, in some circumstances, there can be some variable, weakly positive staining seen with alcian blue, yielding a very pale blue.[6]

Metanil yellow is a counterstain that stains collagen yellow. Some procedures call for the use of saffron (a rather expensive spice); however, for economical purposes, metanil yellow has been substituted for saffron in this report. When the metanil yellow is combined with

Fig. 3A, 3B. Biopsy from the long segment of Barrett's esophagus, 28-40 cm from the incisors, demonstrating the esophageal mucosa. H&E. A) 40X; B) 400X

Fig. 3C, 3D. Biopsy from the long segment of Barrett's esophagus, 28-40 cm from the incisors, demonstrating the presence of specialized intestinal metaplasia. AB-H&E-MY. C) 100X; D) 200X

the alcian blue, the mucin in Barrett's esophagus stains a brilliant turquoise color. In some situations, it can become difficult to determine if the glands present in an esophageal biopsy are gastric mucosa or intestinal metaplasia, as seen in Barrett's esophagus. By using the AB-H&E-MY stain, the cells of Barrett's esophagus are more easily demonstrated.

Case Studies
The following are three case studies that represent the clinical significance of the stain. In all three cases, the pathologist was presented with an H&E at three levels and an

AB-H&E-MY of consecutive sections of the same three levels.

1. A 77-year-old Caucasian male suffers from chronic reflux and has a history of Barrett's esophagus. He also has a small hiatal hernia. The patient was scheduled for a follow-up endoscopic biopsy to determine if dysplasia was present. The biopsy was obtained from the long segment of Barrett's esophagus, 28-40 cm from the incisors. The H&E revealed glandular mucosa with infiltration of plasma cells and lymphocytes, and the biopsy was negative for dysplasia.

Fragments showed ulceration and erosion with the presence of granulation tissue. The presence of specialized intestinal metaplasia was demonstrated by the AB-H&E-MY (Fig. 3C, 3D). The patient was diagnosed with ulceration with erosion and granulation tissue and chronically inflamed, nondysplastic Barrett's esophagus. The patient is recommended to undergo a repeat biopsy in 2 years.

2. A 56-year-old Caucasian male has a history of Barrett's esophagus. His last endoscopic evaluation was 2 years previous, indicating Barrett's esophagus and showing no dysplasia. The patient was scheduled for a follow-up endoscopic biopsy to determine if dysplasia is present. The biopsy was obtained from the long segment of Barrett's esophagus, 25-40 cm from the incisors. The H&E revealed chronically inflamed glandular tissue, with numerous plasma cells and lymphocytes in the lamina propria, and the biopsy was negative for dysplasia. The AB-H&E-MY demonstrated a large number of goblet cells present (Fig. 4C, 4D). The patient was diagnosed with chronic active inflammation of nondysplastic Barrett's esophagus. The patient is recommended to undergo a repeat biopsy in 2 years.

3. A 65-year-old Caucasian female came to the emergency room presenting with symptoms of diarrhea, bloody stool, and tenderness in the lower abdominal area; the symptoms have been present for 10 days and worsen after she eats. She has a history of dysphagia (difficulty swallowing), esophagitis (inflammation of the esophagus), and GERD. The patient was scheduled for an endoscopic biopsy to rule out Barrett's esophagus, and the biopsy was taken from the region of the GE junction. The H&E revealed esophageal mucosa of squamous epithelium that was negative for dysplasia. The gastric mucosa has a large amount of lymphatic infiltrate in the lamina propria. The AB-H&E-MY confirms the presence of focalized intestinal metaplasia (Fig. 5C, 5D). The patient was diagnosed with chronically inflamed, nondysplastic Barrett's esophagus.

Materials and Methods
Tissue Preparation and Sectioning
Hollandes fixative is the preferred fixative for gastrointestinal biopsies. Hollandes is a picric acid-based fixative that is very effective in preserving the mucin in the tissue.[6] However, since mucin does not break down as quickly as other carbohydrates, neutral buffered formalin can be used. Routinely processed paraffin sections are cut at 4 μm, and sections for the routine H&E and the AB-H&E-MY are cut at the same time.

Solutions
3% Acetic Acid
Glacial acetic acid............3.0 ml
Distilled water...............97.0 ml
Stir together. Stable at room temperature for months.

Alcian Blue, pH 2.5
Alcian blue ....1.0 g
3% acetic acid ....100.0 ml
Thymol crystals
Dissolve alcian blue in acetic acid. Check pH; adjust the pH to 2.5, using acetic acid as needed. Add a few crystals of thymol to prevent mold growth. Solution is stable at room temperature for months and may be reused until weak.
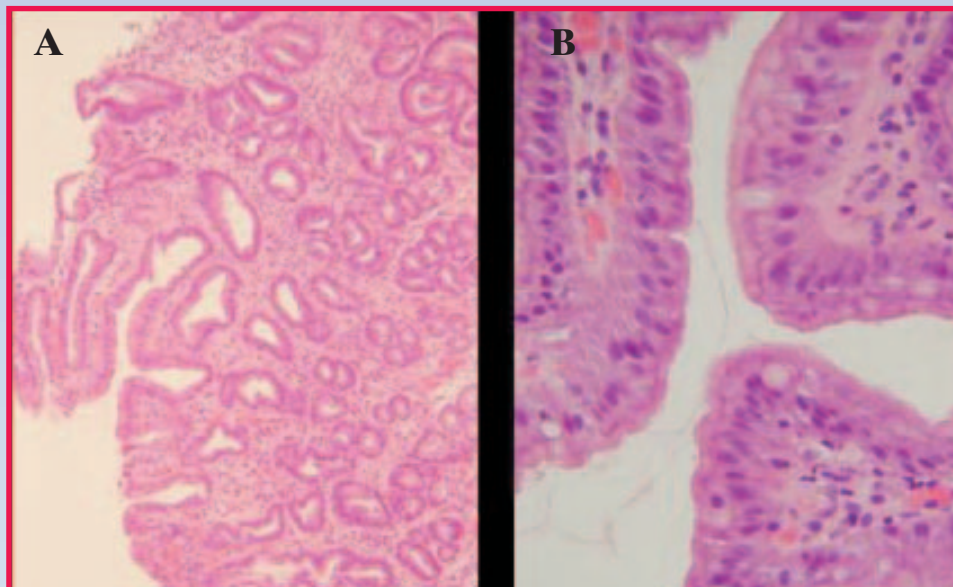
Mayer Hematoxylin
Commercially made

Fig. 4A, 4B. Biopsy from the long segment of Barrett's esophagus, 25-40 cm from the incisors, demonstrating the mucosa. H&E. A) 40X; B) 400X
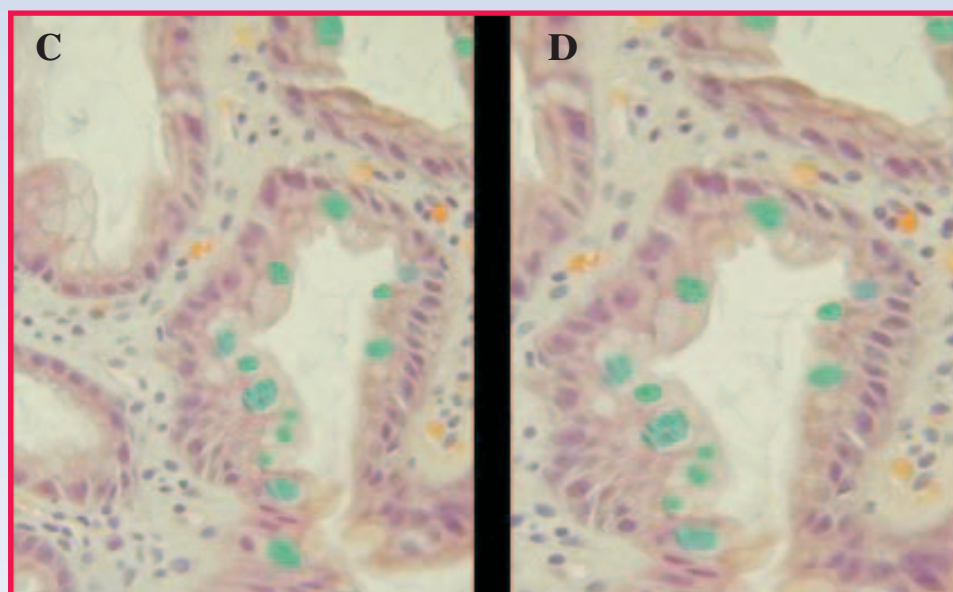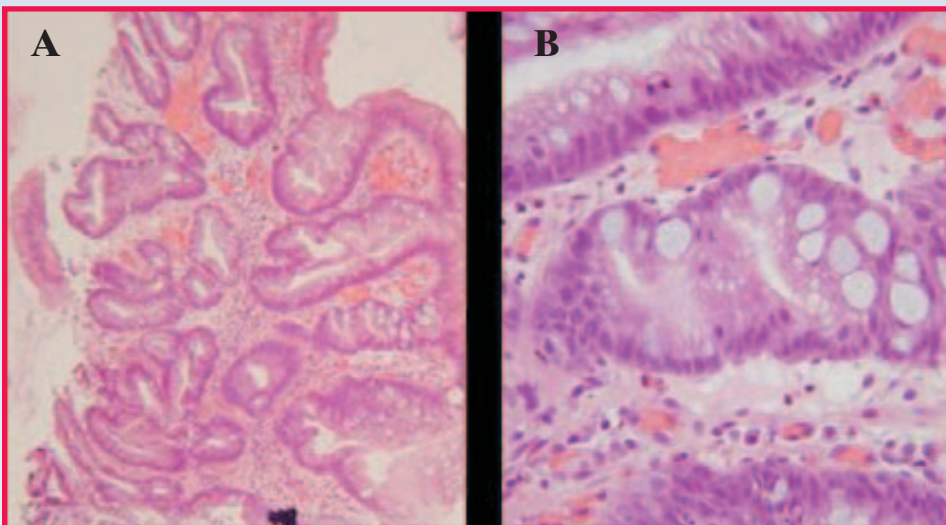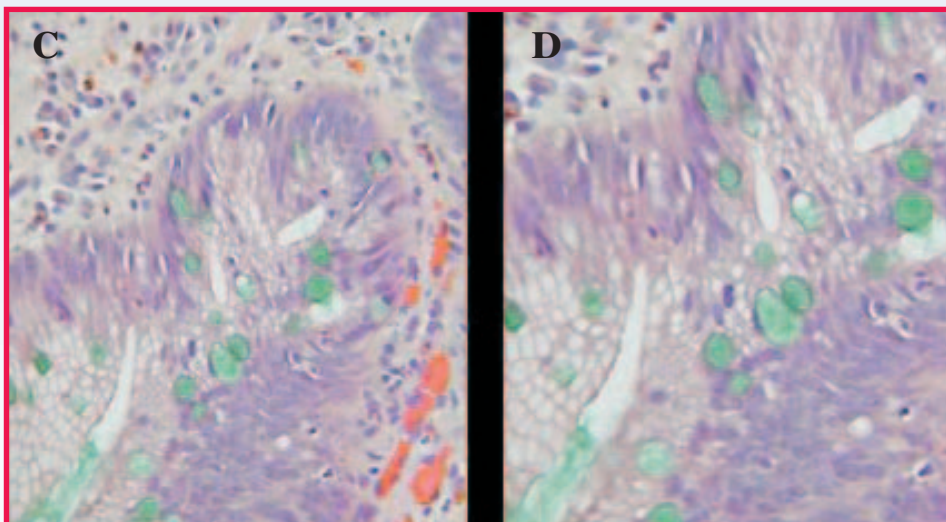

Fig. 4C, 4D. Biopsy from the long segment of Barrett's esophagus, 25-40 cm from the incisors, showing a large number of goblet cells, indicative of intestinal metaplasia in the esophageal mucosa. AB-H&E-MY. C) 100X; D) 400X
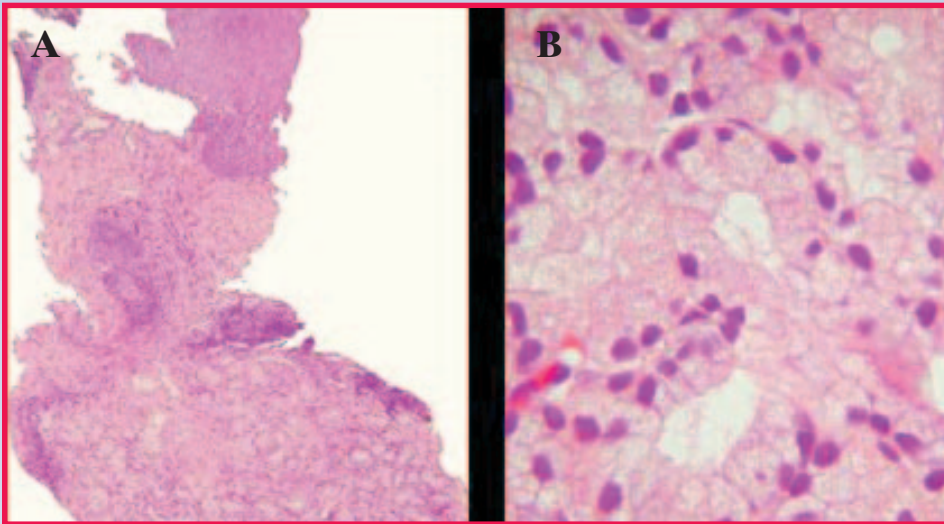
Fig. 5A, 5B. Biopsy from the region of the GE junction, demonstrating esophageal and gastric mucosa. H&E. A) 40X; B) 400X
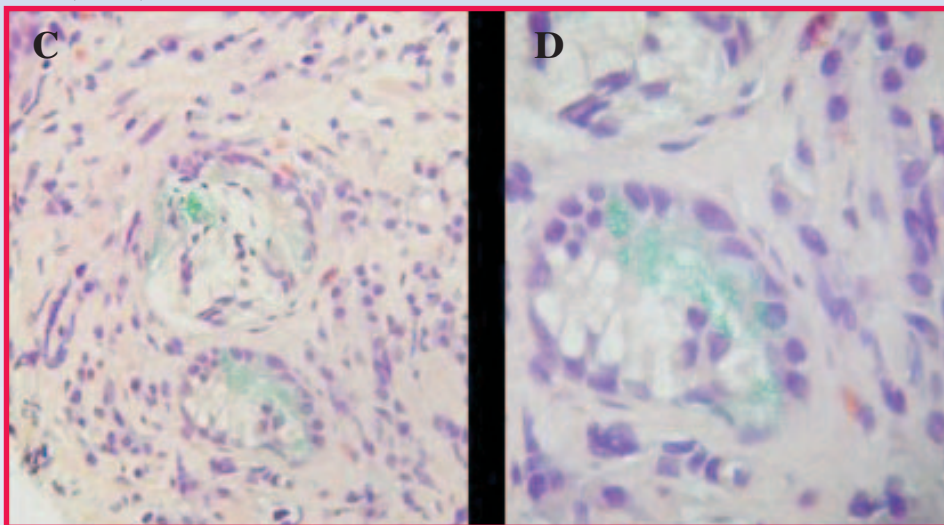

Fig. 5C, 5D. Biopsy from the region of the GE junction, demonstrating the presence of focalized intestinal metaplasia. AB-H&E-MY. C) 100X; D) 400X

0.25% Hydrochloric Acid
Hydrochloric acid, conc. …2.5 ml
Distilled water …………997.5 ml
Carefully add hydrochloric acid to the distilled water slowly. Stable at room temperature for months.

0.25% Ammonia Water
Ammonium hydroxide, conc.1.0 ml
Distilled water …………399.0 ml
Slowly add ammonium hydroxide to distilled water. Use for 1 day only.

Eosin
Commercially made

0.25% Metanil Yellow
Metanil yellow ……………0.25 g
Distilled water …………100.0 ml
Glacial acetic acid ………0.25 ml
Mix together well. Stable at room temperature for up to 1 year.

Method
1. Deparaffinize and bring sections to water
2. Stain with alcian blue, pH 2.5 solution, 15 minutes
3. Wash well with water
4. Stain in Mayer hematoxylin,* 4 minutes
5. Rinse in running water, several changes
6. Differentiate in 0.25% hydrochloric acid, 2-3 seconds
7. Rinse in running water, several changes
8. Blue in 0.25% ammonia water, 2-3 seconds
9. Rinse well in running water, several changes
10. Place in 70% ethanol, 1 minute
11. Stain with eosin solution, 1 minute
12. Dehydrate in 95% ethanol, 30-60 seconds
13. Dehydrate in 100% ethanol, two changes, 30 seconds each
14. Place in metanil yellow solution,† 1 minute
15. Rinse with ethanol, 2 changes, 10 dips each
16. Clear with xylene, 3 changes, 2 minutes each
17. Mount in a resinous medium

*For automated stainers, run a program on the stainer that takes the slides from water, through your routine H&E, and stops at the second change of absolute ethanol.
†Timing of the metanil yellow is critical. If stained for too long, increased background staining will occur.

Results
Nuclei—blue

Cytoplasm—pink-red

Mucin—turquoise for Barrett's esophagus goblet cells (some gastric mucin will stain a faint blue)

Collagen—yellow

Smooth muscle—salmon

Conclusion
When the three stains used in the AB-H&E-MY are combined, they yield dark blue nuclei, pinkish-red cytoplasm, turquoise mucin in Barrett's esophagus vs. either nonstaining or pale blue mucin of herniated tissue, yellow collagen, and salmon smooth muscle. This stain gives the pathologists a colorful demonstration of the various components of the gastrointestinal tract with which to make a diagnosis. It is very useful in diagnosing Barrett's esophagus and distinguishing it from other GI conditions.

References
1. Burkitt HG, Young B, Heath JW. *Wheater's Functional Histology: A Text and Colour Atlas*. 3rd ed. Churchill Livingstone; 1993.
2. Blount PL, Cowan DS, Reid BJ. Fred Hutchinson Cancer Research Center and the University of Washington. An in-depth information source about Barrett's esophagus. Available at: http://barrettsinfo.com/index.htm.
3. Levine DS. Barrett's esophagus. *Sci Am*. 1994;1:16-25.
4. Johns Hopkins Pathology Web site. Barrett's esophagus: understanding Barrett's. Available at: http://pathology2.jhu.edu/beweb/menu_understanding.cfm.
5. Reid BJ, Blount PL, Rubin CE, Levine DS, Haggitt RC, Rabinovitch PS. Flow cytometric and histologic progression to malignancy in Barrett's esophagus: prospective endoscopic surveillance of a cohort. *Gastroenterology*. 1992;102:1212-1219.
6. Bancroft JD, Gamble M. *Theory and Practice of Histological Techniques*. 5th ed. New York, NY: Churchill Livingstone; 2002:163-169, 178-183.

Double Embedding: Double the Trouble?

M. Reid, MLT; C. Goodwin, MLT
Department of Pathology
& Laboratory Medicine
Mount Sinai Hospital
University of Toronto, Canada
mreid@mtsinai.on.ca

Abstract
Traditionally, double embedding[1] is used to process large and dense bone blocks. While the quality of the sections is excellent, there are safety issues to be considered, such as exposure of technologists to chemical fumes. Ether, celloidin, and chloroform can be toxic to the respiratory system. In addition, these chemicals are a fire hazard for the laboratory. Automation of double embedding has been precluded by the use of these hazardous solutions during processing. This lack of automation results in a totally manual procedure, which takes 15 days to complete, increasing the technologist's hands-on time and delaying the time to diagnosis. In the interest of reducing turnaround times and exposure to volatile chemicals, we have developed an automated processing schedule to embed large and dense bone blocks on a standard processor. By using prolonged times in graduated alcohols, xylenes, and paraffin, we have been able to reduce the specimen processing time to 3 days. Blocks embedded using this processing technique demonstrate no difference in cutting, and the histological features of the tissue are preserved. Decreasing turnaround times without sacrificing quality has had a positive impact on the cost of processing and quality of patient care.

Introduction
Cutting large bone blocks presents one of the greatest challenges for the histotechnologist. Every stage of processing must be adequately performed to ensure good quality sections. Double embedding using celloidin has been the method of choice because of its excellent results. There is little shrinkage of the tissue since no heat is used during processing. Tough tissue is not made any harder; soft tissue is completely impregnated and supported; and the relationship of different tissues is maintained.

There are also some disadvantages to double embedding. The ether, celloidin, and chloroform used in processing pose a respiratory danger for the technologist. The chemicals must be used in an adequately ventilated area, preferably a fume hood, which means that this method cannot be automated. Performing each step manually increases the technologist's hands-on time. It takes 15 days to complete the processing from dehydration to wax impregnation. This greatly delays the turnaround time for patient diagnosis. In order to reduce both the turnaround time and exposure of the technologist to hazardous chemicals used in double embedding, we set out to develop an automated processing method that maintains the histological appearance but shortens the processing time.

Materials and Methods
Representative 5 mm thick sections were sampled from human femoral head, tibial plateau, and femur (cross-section). The tissues varied in size from 2x2 to 5x5 cm in cross-section. The tissues were fixed in 10% buffered formalin (0.1M phosphate buffer, pH 7.4) (VWR, Ontario, Canada) for 48 hours. All blocks were decalcified in

Table 1
DOUBLE EMBEDDING SCHEDULE

70% alcohol	72 hours	21°C
100% alcohol	24 hours	21°C
100% alcohol	24 hours	21°C
100% alcohol	24 hours	21°C
50% ether/alcohol	24 hours	21°C
1%-2% celloidin in ether alcohol	72 hours	21°C
Chloroform	24 hours	21°C
100% xylene	24 hours	21°C
100% xylene	24 hours	21°C
Paraplast®* X-tra wax	24 hours	21°C
Paraplast X-tra wax	24 hours	21°C
Embed in Paraplast X-tra wax		

Table 2
AUTOMATED PROCESSING SCHEDULE

70% alcohol	18 hours	35°C	No vacuum	Agitation on
90% alcohol	3 hours	35°C	No vacuum	Agitation on
100% alcohol	3 hours	35°C	No vacuum	Agitation on
100% alcohol	3 hours	35°C	No vacuum	Agitation on
100% alcohol	3 hours	35°C	No vacuum	Agitation on
100% alcohol	3 hours	35°C	No vacuum	Agitation on
100% xylene	4 hours	35°C	No vacuum	Agitation on
100% xylene	5 hours	35°C	No vacuum	Agitation on
Paraplast wax	4 hours	60°C	No vacuum	Agitation on
Paraplast wax	3 hours	60°C	No vacuum	Agitation on
Paraplast wax	3 hours	60°C	No vacuum	Agitation on
Paraplast X-tra wax	6 hours	60°C	No vacuum	Agitation on
Embed in Paraplast X-tra wax				

*Paraplast is manufactured by Tyco Healthcare/Kendall, Mansfield, MA.

8% formic acid (pH 2.0) (Fisher Scientific Co., Ltd., Toronto, Canada) until decalcified. This was determined by gross examination. One set of blocks was processed using the double embedding method (Table 1). The adjacent sections were processed using an automated method on a Tissue-Tek® VIP™ Processor (Sakura Finetek, Torrance, CA) (Table 2). The methods are detailed in Tables 1 and 2.

Results

After processing, the integrity of the bone samples was maintained. There was no difference noted in the ease of sectioning the blocks, and all blocks were able to produce ribbons. There was no distortion or significant shrinkage observed in the tissue or the sections obtained from blocks that were processed using the automated cycle, compared to the sections from the double embedded blocks. Light microscopy examination demonstrated that the histological appearance of tissue sections from blocks processed using the automated method (Fig. 1C, 1D) were preserved and appeared identical to those seen in tissue sections from blocks processed by the double embedding method (Fig. 1A, 1B).

The processing time was reduced from 15 days using the double embedding schedule to 3 days using the automated processing schedule. The technologist's hands-on time was decreased approximately tenfold using the automated schedule. Eliminating the use of chloroform, ether, and celloidin also reduced the technologist's exposure to dangerous fumes, with no obvious effects on histology.

Conclusions

1) A long automated processing cycle can replace the double embedding method for large and dense bone blocks.

2) This method decreased processing turnaround time fivefold and should impact favorably on the length of time to diagnosis.

3) There was reduced chemical exposure for technologists, as potentially harmful chemicals were eliminated.

Reference

1. Bancroft JD, Gamble M. *Theory and Practice of Histological Techniques.* 5th ed. New York, NY: Churchill Livingstone; 2002:281.
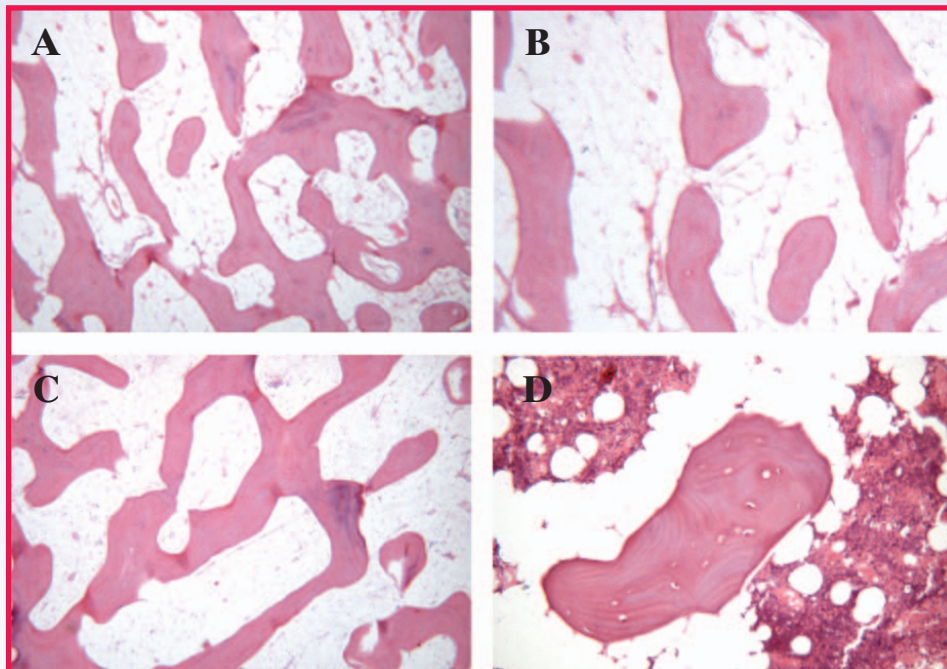
Fig. 1. Histological sections of decalcified bone that have been processed either by the double embedding method (A, B) or the long automated schedule (C, D). There is no difference in the histological appearance of the bone. Hematoxylin and eosin: A and C, 40X; B and D, 250X

√ Mark Your Calendar! Educational Opportunities in 2005

January 19   **National Society for Histotechnology**
Teleconference 1:00 pm Eastern Time
(301) 262-6221
Title: **"Mohs Histographic Surgery for Histologists"**
Speaker: Clifford Chapman, HTL(ASCP)QIHC

January 21   **University of Texas Health Sciences Ctr/ San Antonio**
Teleconference 12:00 pm Central Time
(800) 982-8868
Title: **"Basic Principles of Fixation"**
Speaker: Barry Rittman, PhD

February 16   **National Society for Histotechnology**
Teleconference 1:00 pm Eastern Time
(301) 262-6221
Title: **"QC, QA and QI: Qualifiers, Quirks and Questions"**
Speaker: Sandra Dolar, BA, CT(ASCP)

February 18   **University of Texas Health Sciences Ctr/ San Antonio**
Teleconference 12:00 pm Central Time
(800) 982-8868
Title: **"Packaging Regulations for Diagnostic Specimens Have Changed Again"**
Speaker: Linda Durbin, President
EXAKT Technologies, Inc.
Oklahoma City, OK

March 3-5   **Indiana Society for Histotechnology**
Site: Downtown Hilton, Indianapolis, IN
Contact: LaDonna Elpers (812) 985-5900 ext 128
Email: lelpers@bioanalytical.com

March 16   **National Society for Histotechnology**
Teleconference 1:00 pm Eastern Time
(301) 262-6221
Title: **"Grossing Procedures for the Histotech"**
Speaker: Michael LaFriniere, PA, HT(ASCP)

March 18   **University of Texas Health Sciences Ctr/ San Antonio**
Teleconference 12:00 pm Central Time
(800) 982-8868
Title: **"Dermatopathology: Histology and Surgical Grossing"**
Speaker: Clifford M. Chapman, MS, HTL(ASCP),QIHC

March 18-19   **Kentucky Society for Histotechnology**
Site: Louisville, KY
Contact: Renee Matherly (502) 852-5587
Email: rmath0516@aol.com

March 26   **Massachusetts Society of Histotechnology**
Site: Fenway Park, Boston, MA
Contact: Jason Burrill (978) 658-6000 x1229
Email: jburrill@criver.com

April 15   **University of Texas Health Sciences Ctr/ San Antonio**
Teleconference 12:00 pm Central Time
(800) 982-8868
Title: **"Immunohistochemical Staining Techniques to Localize *Treponema pallidum* Spirochetes"**
Speaker: Hazel V. Dalton, BA, HT, QIHC (ASCP)

April 15-16   **Region I Symposium**
Site: Doubletree Hotel, Windsor Locks, CT
Contact: Jason Burrill (978) 658-6000 x1229
Email: jburrill@criver.com

April 20   **National Society for Histotechnology**
Teleconference 1:00 pm Eastern Time
(301) 262-6221
Title: **"Prions: Working With Infectious Proteins"**
Speakers: Lisa Manning, BS, RT
and Stefanie Czub, DVM

April 21-24   **Texas Society for Histotechnology**
Site: Marriott Dallas/Plano at Legacy Town Center
Contact: Donna Willis (817) 878-5644
Email: donnawillis@texashealth.org

April 22-23   **Region VII & Colorado Society of Histotechnology**
Site: Beaver Run Resort, Breckenridge, CO
Contact: John McGinley (970) 491-3041
Email: john.mcginley@colostate.edu
Web: www.coloradohisto.org

April 22-23   **North Carolina Society for Histopathology Technologists**
Site: Greensboro Airport Marriott
Contact: Delorise Williams, President (919) 558-1200
Email: dwilliams@ciit.org

April 27-29   **Wisconsin, Minnesota, Iowa (Tri-State Symposium)**
Site: Radisson, Rochester, MN
Contact: Sue Ubl (608) 262-5432
Email: sue.ubl@wudl.wisc.edu

April 29-30   **Region I Symposium**
Site: Quality Inn, Vernon, CT
Contact: Denise Woodward (860) 429-5163
Email: dlongwoodward@charter.net

April 30 - May 1   **Washington State Histology Symposium**
Site: Washington Athletic Club, Seattle, WA
Contact: Linda Cherepow (206) 667-1378
Email: lcherepo@fhcrc.org

May 6-7   **New York State Histological Society**
Site: Holiday Inn, Binghamton, NY
Contact: Judy LaDuc (518) 897-2247
Email: jaladuc@capital.net

May 12-13   **Illinois Society for Histotechnologists State Meeting**
             Site: Peoria, IL
             Contact: Dana Spears (309) 344-2451
             Email: dspears@agr.state.il.us

May 18   **National Society for Histotechnology**
             Teleconference 1:00 pm Eastern Time
             (301) 262-6221
             Title: **"Mastering the Trichrome Stain—**
                        From Troubleshooting to Diagnosis"
             Speaker: M. Lamar Jones, BS, HT(ASCP)

May 20   **University of Texas Health Sciences Ctr/**
             San Antonio
             Teleconference 12:00 pm Central Time
             (800) 982-8868
             Title: **"Specimen Preparation for Laser**
                        Microdissection (LCM)"
             Speaker: Diane L. Sterchi, MS, HT/HTL
                        (ASCP), EM (MSA)

May 20-21   **Michigan Society**
             Site: Traverse City Park Place Hotel
                        Traverse City, MI
             Contact: Paula Bober (313) 729-1891
             Email: pbober@dmc.org

June 3-4   **Louisiana Society of Histotechnology**
             Site: Wyndham Metairie-New Orleans
                        Metairie, LA
             Contact: Jane Goodman (504) 897-8830
             Email: jan715387@aol.com

June 15   **National Society for Histotechnology**
             Teleconference 1:00 pm Eastern Time
             (301) 262-6221
             Title: **"Tissue Microarrays"**
             Speakers: Wanda Jones, HT(ASCP)
                        and Paul Billings

June 17   **University of Texas Health Sciences Ctr/**
             San Antonio
             Teleconference 12:00 pm Central Time
             (800) 982-8868
             Title: **"Decalcified Bone Sections**
                        in Animal Models of Osteoarthritis"
             Speaker: Elizabeth A. Chlipala, BS,
                        HTL(ASCP)QIHC

July 15   **University of Texas Health Sciences Ctr/**
             San Antonio
             Teleconference 12:00 pm Central Time
             (800) 982-8868
             Title: **"Quick Fix: Safe Handling**
                        of Histological Fixatives"
             Speaker: Maureen Doran, BA, HTL(ASCP)

July 20   **National Society for Histotechnology**
             Teleconference 1:00 pm Eastern Time
             (301) 262-6221
             Title: **"Immunohistochemical Panels**
                        in Dermatopathology"
             Speaker: David Tacha, PhD, HT(ASCP)

August 19   **University of Texas Health Sciences Ctr/**
             San Antonio
             Teleconference 12:00 pm Central Time
             (800) 982-8868
             Title: **"What Every Histotech**
                        Should Know About Water"
             Speaker: Ethel Macrea, AA, HT(ASCP), QIHC

September 10-14   **NATIONAL SOCIETY**
                  FOR HISTOTECHNOLOGY
                  SYMPOSIUM/CONVENTION
                  Site: Fort Lauderdale, FL
                  Contact: NSH Office
                             4201 Northview Drive, Suite 502
                             Bowie, Maryland 20716-2604
                             (301) 262-6221
                  Fax: (301) 262-9188
                  Email: histo@nsh.org

September 16 **University of Texas Health Sciences Ctr/**
             San Antonio
             Teleconference 12:00 pm Central Time
             (800) 982-8868
             Title: **"Microwave Usage in Today's**
                        Histology Lab"
             Speaker: Donna Willis, HT/HTL(ASCP)

October 21   **University of Texas Health Sciences Ctr/**
             San Antonio
             Teleconference 12:00 pm Central Time
             (800) 982-8868
             Title: **"The Biology of Cancer"**
             Speaker: Jerry Santiago, BS, HTL
                        (ASCP)QIHC

November 5   **Connecticut Society of Histotechnologists**
             TBA
             Contact: Denise Long Woodward (860) 429-5163
             Email: dlongwoodward@charter.net

November 16 **National Society for Histotechnology**
             Teleconference 1:00 pm Eastern Time
             (301) 262-6221
             Title: **"Ionizing Radiation Safety**
                        in the Histology Laboratory"
             Speaker: Cheryl Culver-Schultz, MS

November 18 **University of Texas Health Sciences Ctr/**
             San Antonio
             Teleconference 12:00 pm Central Time
             (800) 982-8868
             Title: **"Handling Bone Specimens"**
             Speakers: Gillian Rittman, ONC
                        and Barry Rittman, PhD

To receive your own copy of **HistoLogic**,® or to have someone added to the mailing list, submit home address to: Sakura Finetek U.S.A., Inc., 1750 West 214th Street, Torrance, CA 90501.

The editor wishes to solicit information, questions, and articles relating to histotechnology. Submit these to: Vinnie Della Speranza, **HistoLogic**® Editor, 165 Ashley Avenue, Suite 309, Charleston, SC 29425. Articles, photographs, etc, will not be returned unless requested in writing when they are submitted.

Sakura Finetek U.S.A., Inc.
1750 West 214th Street
Torrance, CA 90501

HISTOLOGIC®
Technical Bulletin for Histotechnology